NACA RM A51I04

JAN 7 1952

CLASSIFICATION CHANGED

NACA

RESEARCH MEMORANDUM

METHOD FOR ESTIMATING LIFT INTERFERENCE OF WING-BODY

COMBINATIONS AT SUPERSONIC SPEEDS

By Jack N. Nielsen and George E. Kaattari

Ames Aeronautical Laboratory
Moffett Field, Calif.

Made Unavailable by administrative action per
Hdqrs. let. dtd. 3-7-58 signed by B.A. Mulcahy

NATIONAL ADVISORY COMMITTEE
FOR AERONAUTICS
WASHINGTON
December 31, 1951   UNAVAILABLE

NATIONAL ADVISORY COMMITTEE FOR AERONAUTICS

RESEARCH MEMORANDUM

METHOD FOR ESTIMATING LIFT INTERFERENCE OF WING-BODY

COMBINATIONS AT SUPERSONIC SPEEDS

By Jack N. Nielsen and George E. Kaattari

SUMMARY

The modified slender-body method used by Nielsen, Katzen, and Tang in RM A50F06, 1950, to predict the lift and moment interference of triangular wing-body combinations has been adapted to combinations with other than triangular wings. That part of the method for predicting the effect of the body on the wing has been retained, but a new method for predicting the effect of the wing on the body has been presented. These methods have been applied to the prediction of the lift-curve slopes of nearly 100 triangular, rectangular, and trapezoidal wing-body configurations. The estimated and experimental values for the lift-curve slopes agree for most of the cases within ±10 percent. Some of the higher-order effects that must be taken into account in a theory that is to give greater accuracy than the present one are discussed. A numerical example illustrating the method is included.

INTRODUCTION

By properly designing supersonic aircraft and missiles to take advantage of the effects of aerodynamic interference, it may be possible to obtain large increases in performance and efficiency. For this reason, much effort has been expended in trying to predict and control interference effects. One of the most important problems is that of interference between wing and body, and a number of methods have been developed for predicting the characteristics of wing-body combinations at supersonic speeds. These methods generally fall into two categories. The first includes those theories attempting to solve mathematically the complicated boundary-value problems of wing-body interference, and the second category includes those approximate methods based on highly simplifying assumptions. In general, the mathematical theories of the first category are too difficult or time consuming to be useful in ordinary design work. The approximate theories of the second category are

.restricted in scope or are based on assumptions the validity of which
is unknown. As a consequence of these shortcomings, there is a lack at
the present time of a simple, reliable method of calculating wing-body
interference applicable to a wide range of wing-body combinations. It
is the purpose of this report to supply such a method for predicting
lift.

One of the first attempts to solve one of the mathematically com-
plicated boundary-value problems of wing-body interference is that of
Ferrari (reference 1). By assuming the wing to be acting in the field
of the body alone, Ferrari was able to obtain a first approximation to
the pressure field acting on the wing of a rectangular wing-body combi-
nation. By assuming the body to be acting in the field of the wing
alone, Ferrari also obtained the approximate pressure field acting on
the body. In reference 2, Nielsen and Matteson present a calculative
technique for solving wing-body problems of symmetrical configurations.
In reference 3, Moskowitz and Maslen have applied the method to deter-
mining both thickness and lifting pressure distributions of a triangular
wing-body combination and a rectangular wing-body combination, and they
have found good agreement with experiment except in the wing-body junc-
ture, where boundary-layer effects are important. Two other mathemati-
cal attempts to solve boundary-value problems associated with rectangu-
lar wing-body combinations are contained in references 4 and 5. In
reference 4, Morikawa solves approximately the problem of a rectangular
wing on a circular body both at the same angle of attack. In
reference 5, Nielsen presents a general method of solving wing-body
problems for which the interaction between upper and lower wing surfaces
has no effect on the wing-body interference. The case of a rectangular
wing mounted at incidence on a body at zero angle of attack is studied
in detail.

Several approximate theories exist which illustrate important
interference effects. For instance, the theory of Stewart and
Meghreblian in reference 6 accounts for the increased wing lift of the
exposed wings due to body upwash. The authors, however, take no account
of loss of lift behind the Mach cone from the leading edge of the junc-
ture nor of the lift carried over onto the body by the wing. Another
approximate theory is that presented by Morikawa (reference 7) for tri-
angular, rectangular, and trapezoidal wings with no afterbody. While
the limitation to no afterbody is unnecessarily restrictive, the valid-
ity of Morikawa's assumptions for various combinations awaits experi-
mental verification.

An approximate method for triangular wing-body combinations that
has been substantiated by experiment is that of Nielsen, Katzen, and
Tang (reference 8). The possibility of extending this method to combi-
nations with wings of other plan forms mounted on bodies of revolution
is investigated in this report.

SYMBOLS

A   aspect ratio of exposed wing panels joined together

$\bar{c}$ mean aerodynamic chord $\left(\dfrac{\int_r^{s_m} c_y{}^2 dy}{\int_r^{s_m} c_y\, dy} \right)$, inches

C_L lift coefficient based on exposed wing area

$C_{L\alpha}$ lift-curve slope based on exposed wing area

c_r chord at wing-body juncture, inches

c_t wing tip chord, inches

c_y wing chord at spanwise distance y from body axis, inches

d   body diameter, inches

E   complete elliptic integral of second kind

K   ratio of lift of combination to that of wing alone

K_B ratio of lift carried by body of combination to lift acting on wing alone

K_W ratio of lift carried by wing of combination to lift acting on wing alone

L   lift force, pounds

l_a afterbody length, inches

l_f forebody length, inches

M   free-stream Mach number

m   cotangent of leading-edge sweep angle

q   free-stream dynamic pressure, pounds per square inch

r   body radius, inches

R   Reynolds number based on mean aerodynamic chord

S   area of wing alone formed by joining exposed wing panels together, square inches

s_m semispan of wing-body combination, inches

x,y,z   streamwise, spanwise, and vertical coordinates, respectively

α_B angle of attack of body, radians

α_y local angle of attack at spanwise distance   y   from body axis, radians

β $\sqrt{M^2 - 1}$

βA effective aspect ratio

$\dfrac{\beta d}{c_r}$ effective diameter, root-chord ratio

$\Lambda_{L.E.}$ leading-edge sweep angle, degrees

λ taper ratio $\left(\dfrac{c_t}{c_r}\right)$

φ potential of perturbation velocities

Subscripts

W   wing alone

C   wing-body combination

N   nose of combination

C-N   wing-body combination minus nose

B   body alone

W(B)   wing in presence of body

B(W)   body in presence of wing minus body nose

Superscripts

s   slender-body theory

u   upwash theory

ANALYSIS

Observations Concerning Slender-Body Theory

The linearized equation of supersonic wing theory (or wing-body theory) is the wave equation for the velocity potential

$$(M^2 - 1)\ \varphi_{xx} - \varphi_{yy} - \varphi_{zz} = 0 \tag{1}$$

For slender wing-body combinations, Spreiter (reference 9) has shown that the first term of this equation can be ignored so that it reduces to Laplace's equation in the y, z plane. Using this simplification, Spreiter has obtained simple, closed expressions for the lift-curve slopes of many wing-body combinations.

It is well-known that for wing-body combinations which are not slender the lift-curve slopes are overestimated by slender-body theory (reference 8). However, this fact does not preclude the use of slender-body theory for nonslender configurations since, in certain instances, the ratio of the lift of the wing-body combination to that of the "wing alone" may be accurately predicted by slender-body theory, even though the magnitude of the lift-curve slope may be incorrect. From the foregoing ratio and a good estimate of the wing-alone lift-curve slope, the lift-curve slope of the combination can be obtained. This was essentially the method used by Nielsen, Katzen, and Tang in reference 8 to predict the lift and moment characteristics of triangular wing-body combinations. Good agreement between experiment and theory was obtained. The method is limited in principle to those configurations for which slender-body results are available. This means that swept-forward leading edges or swept-back trailing edges are generally precluded.

The success of this method with triangular wing-body combinations was the result of two fortunate circumstances. First, the assumptions of slender-body theory are best met for combinations in which the lateral dimensions expand slowly, as for triangular wing-body combinations. Also, because the aspect ratio of the wing alone is the same whether the wing alone is defined as the exposed half-wings joined together or as the triangular wing that includes the area of the wing blanketed by the body, the method of reference 8 gives identical results for the

lift-curve slope using either definition. However, for wing-body combinations employing other than triangular wings, the wing-alone aspect ratio depends on the wing-alone definition. Thus the application of the method of reference 8 to rectangular wing-body combinations was found to give significantly different results, depending on whether the wing alone was taken as the exposed half-wings joined together or as the exposed half-wings plus the blanketed area. Although an attempt to determine a percent effective blanketed area was partially successful, this quantity depended on βA and $\beta d/c_r$, and for other wing plan forms would depend on additional parameters. This difficulty made it necessary to attack the problem from an entirely different point of view from that of reference 8. The method of Morikawa (reference 7) for presenting lift interference was adopted.

In presenting the lift results use is made of a number of wing-body parameters. A wing plan form with trapezoidal panels of uniform taper can be specified entirely by aspect ratio, taper, and cotangent of the leading-edge sweep angle. For supersonic flow, the effective values of these parameters are βA, λ, and βm. An additional parameter relating body size to some characteristic wing dimension is required to characterize completely the geometry of a wing-body combination. The parameters r/s_m and $\beta d/c_r$ are both used for this purpose.

In the method of Morikawa for presenting lift interference, the wing alone is defined as the exposed half-wings joined together. The lift of the wing-body combination exclusive of the forebody is related to the lift of the wing alone by the factor K which is to be determined.

$$L_{C-N} = K L_W \tag{2}$$

The factor K is decomposed into two factors K_B and K_W which represent the ratios of the body lift and wing lift of the combination to that of the wing alone.

$$K = K_B + K_W \tag{3}$$

$$K_B = \frac{L_{B(W)}}{L_W} \tag{4}$$

$$K_W = \frac{L_{W(B)}}{L_W} \tag{5}$$

So far, the scheme is only a way of representing lift results. The solution of the problem requires a determination of values of K_W and K_B that are reliable for all wing aspect ratios. In his paper,

Morikawa has given the slender-body values of K, K_W, and K_B which will be indicated here by a superscript.

$$K^{(s)} = \left(1 + \frac{r}{s_m}\right)^2 \tag{6}$$

where r is the body radius and s_m is the maximum wing semispan. (The assumption is made that no negative lift is developed behind the maximum wing span. R. T. Jones (reference 10) has pointed out that for wings, at least, the negative lift predicted on these sections by slender-body theory is prevented by separation.) The value of $K_W^{(s)}$ given by the slender-body theory is

$$K_W^{(s)} =$$

$$\frac{2}{\pi} \frac{\left\{\left(1+\frac{r^4}{s_m^4}\right)\left[\frac{1}{2}\tan^{-1}\frac{1}{2}\left(\frac{s_m}{r}-\frac{r}{s_m}\right)+\frac{\pi}{4}\right]-\frac{r^2}{s_m^2}\left[\left(\frac{s_m}{r}-\frac{r}{s_m}\right)-2\tan^{-1}\frac{s_m}{r}+\pi\right]\right\}}{\left(1-\frac{r}{s_m}\right)^2} \tag{7}$$

The value of $K_B^{(s)}$ is obtained by subtraction. A plot of $K^{(s)}$, $K_W^{(s)}$, and $K_B^{(s)}$ as determined by slender-body theory appears in figure 1. In the limiting case of $r/s_m = 0$ the combination is all wing and the value of $K_W^{(s)} = 1$ and $K_B^{(s)} = 0$. As r/s_m approaches unity, there is a very small exposed wing. For this small wing, the body is effectively a vertical reflection plane and the angle of attack is 2α due to upwash (as will be discussed later). This makes $K_W^{(s)} = 2$. The wing produces an equal amount of lift on the body.

It is clear that the values of $K_B^{(s)}$ and $K_W^{(s)}$ should be satisfactory for slender wing-body combinations. However, they cannot be used for large aspect ratios for which slender-body theory is inapplicable without further investigation. Independent methods of determining K_B and K_W will now be presented, and the applicability of $K_B^{(s)}$ and $K_W^{(s)}$ will be inferred by comparison.

Increase in Wing Lift Due to Body Upwash

An approximate method for evaluating K_W is to suppose that the exposed wings are operating in the upwash field of the body alone and then to calculate the resultant wing lift. Neglecting any effect of the nose, it has been pointed out (reference 11) that the upflow angle due to the body varies spanwise on the horizontal plane of symmetry as

$$\alpha_y = \alpha_B \left(1 + \frac{r^2}{y^2} \right) \tag{8}$$

where y is the lateral distance from the body axis. The wing is thus effectively twisted by the body-alone flow. If now the upwash angle given by equation (8) is taken into account by using strip theory, an approximate value of K_W is obtained as follows:

$$K_W(u) = \frac{\displaystyle\int_r^{s_m} \alpha_y\, c_y\, dy}{\alpha_B \displaystyle\int_r^{s_m} c_y\, dy} \tag{9}$$

Equation (9) does not include tip effects. The following expression is obtained in terms of r/s_m and taper for wings of uniform taper.

$$K_W(u) = \frac{\frac{1}{2}(1+\lambda) - \frac{\lambda r}{s_m} - \frac{r^2(1-\lambda)}{s_m{}^2 - r^2} \ln\left(\frac{s_m}{r}\right)}{\frac{1}{2}\left(\frac{s_m - r}{s_m + r}\right)(1+\lambda)} \tag{10}$$

It is notable that $K_W{}^{(u)}$ does not depend on aspect ratio.

Equation (10) was used to determine $K_W{}^{(u)}$ for $\lambda = 0, \frac{1}{2}$, and 1, and these results are compared to those of slender-body theory in figure 2. It is seen that the effect of taper is small compared to the effect of r/s_m. Both theories give nearly the same values at both high and low values of r/s_m, but the values of $K_W{}^{(u)}$ are in all instances greater than $K_W{}^{(s)}$. Nowhere is the difference of great significance. Although account has been taken of the upwash induced along the wing span by the body in the determination of $K_W{}^{(u)}$, no account has been taken of the loss of lift due to interaction between the wing and the body of the winged part of the combination. For this reason, $K_W{}^{(u)}$ will be too large. Therefore, it was decided to use $K_W{}^{(s)}$ for all

combinations. This procedure corresponds to the method of reference (8)
with the wing alone defined to be the exposed half-wings joined together.

Lift Carried Onto Body From Wing

While the upwash theory represents a simple method for estimating
the effect of the body in increasing the wing lift, no general, simple
method, other than slender-body theory, exists for estimating the lift
carried onto the body by the wing. Morikawa, in reference 7, has esti-
mated K_B for combinations with no afterbody using various assumptions
for various plan forms. A method using uniform assumptions and includ-
ing afterbody effects will now be given.

On the basis of slender-body theory, nonexpanding sections of a
body in a uniform flow develop no lift. Therefore, the lift on a
straight portion of a body on which a wing is mounted is due princi-
pally to lift carried over from the wing onto the body. A point on the
wing is thought of as a source of lifting disturbances which move in all
directions in the downstream Mach cone from the point. Some of these
disturbances are carried over onto the body. The assumption is made
that the sole effect of the body (regardless of cross section) is to dis-
place these pulses downstream without diminishing their lifting poten-
tial. This is the so-called delayed reaction of Lagerstrom and Van Dyke
in reference 12, which was substantiated for a particular family of rec-
tangular wing-body combinations by Nielsen in reference 5. Downstream
of the wing, the flow returns to the free-stream direction. The effect
of this change in flow direction is felt on the surface of the afterbody
behind the Mach helix originating at the trailing-edge, root-chord junc-
ture. In this region, the reaction tends to cancel the lift carried
over from the wing onto the body. The effective resultant lifting area
on the body for one half-wing can thus be approximated by the shaded
area shown in figure 3(a).

While a nonplanar model has been set up to represent the lift car-
ried over onto the body by the wing, further simplification to an equiv-
alent planar case is desirable before calculations can be performed.
The body is imagined now to be collapsed to a plane and the Mach helices
of figure 3(a) become the Mach lines of figure 3(b). The lifting area
of the body is the shaded area of figure 3(b) at zero angle of attack.
This area is equal to the horizontal projection of the lifting area of
the actual body surface (fig. 3(a)). The lift on the body can be calcu-
lated simply by integrating pressures due to the half-wing over the
shaded area and doubling the result.

In determining the pressure field of the half-wing on the planar
area, both subsonic and supersonic leading edges are considered. Tip

effects are not considered, and the analysis is confined to the case in which the Mach line emanating from the leading edge of the wing tip falls behind the region of lift carry-over onto the body. This condition imposes the following restriction:

$$\beta A \, (1+\lambda)\left(\frac{1}{\beta m} + 1\right) \geq 4 \tag{11}$$

on the wings for which the method is to apply.

The value of lift carried over onto the body by a half-wing with a supersonic leading edge is given (using the solution of reference 13) as

$$L = \frac{4q\alpha_W}{\beta\pi} \frac{\beta m}{\sqrt{\beta^2 m^2 - 1}} \int_0^d d\eta \int_\eta^{c_r+\eta} \cos^{-1}\frac{\frac{\xi}{\beta} + \beta m\eta}{(\eta+m\xi)} d\xi \tag{12}$$

with the coordinate system of figure 3(b). This result is doubled to account for the lift of two half-wings and divided by the lift of the wing alone to obtain K_B. For all Mach numbers K_B is

$$K_B = \frac{8\beta m}{\pi \sqrt{\beta^2 m^2 - 1}\,(1+\lambda)\left(\beta\frac{d}{c_r}\right)\left(\frac{s_m}{r} - 1\right)\left(\beta C_{L_\alpha}\right)_W}$$

$$\left\{\left(\frac{\beta m}{1+\beta m}\right)\left[\frac{(\beta m+1)\frac{\beta d}{c_r}+\beta m}{\beta m}\right]^2 \cos^{-1}\left[\frac{1+(1+\beta m)\beta\frac{d}{c_r}}{\beta m+(\beta m+1)\frac{\beta d}{c_r}}\right] + \frac{\sqrt{\beta^2 m^2 - 1}}{(\beta m+1)}\left[\sqrt{1+2\frac{\beta d}{c_r}} - 1\right] - \right.$$

$$\left. \frac{\sqrt{\beta^2 m^2 - 1}}{\beta m}\left(\frac{\beta d}{c_r}\right)^2 \cosh^{-1}\left(1 + \frac{c_r}{\beta d}\right) - \frac{\beta m}{1+\beta m}\cos^{-1}\left(\frac{1}{\beta m}\right)\right\} \tag{13}$$

where $m\beta > 1$.

Similarly, for subsonic leading edges there is obtained, using the appropriate conical lifting solution from reference 14,

$$L = \frac{8q\alpha_w(\beta m)^{3/2}}{\pi\beta(\beta m+1)} \int_0^d d\eta \int_\eta^{c_r+\eta} \frac{\sqrt{\dfrac{\xi}{\beta} - \eta}}{\sqrt{m\xi+\eta}} \, d\xi \qquad (14)$$

giving

$$K_B = \frac{16\left(\dfrac{\beta m}{1+m\beta}\right)^2}{\pi\,(1+\lambda)\left(\dfrac{\beta d}{c_r}\right)\left(\dfrac{s_m}{r}-1\right)\left(\beta C_{L_\alpha}\right)_W}$$

$$\left\{ \left[\frac{\beta m+(1+m\beta)\dfrac{\beta d}{c_r}}{\beta m}\right]^{3/2} + \left[\frac{\beta m+(1+m\beta)\dfrac{\beta d}{c_r}}{\beta m}\right]^{1/2} - \right.$$

$$\left. 2 - \left[\frac{(1+m\beta)\dfrac{\beta d}{c_r}}{m\beta}\right]^2 \tanh^{-1}\sqrt{\frac{\beta m}{\beta m+(1+m\beta)\dfrac{\beta d}{c_r}}} \right\} \qquad (15)$$

where $m\beta < 1$.

The effect of body upwash in increasing the lift of the exposed wing has not been taken into account in calculating the effect of the wing on the body.

It is to be noted that K_B in equations (13) and (15) depends on a number of parameters, of which four are independent. However, the quantity $K_B(1+\lambda)\left(\dfrac{s_m}{r}-1\right)\left(\beta C_{L_\alpha}\right)_W$ is a function of only $m\beta$ and $\dfrac{\beta d}{c_r}$. The quantity is presented as a function of $\beta d/c_r$ for constant values of $m\beta$ in figure 4 which is to serve as a design chart in determining K_B subject to the restriction of equation (11). The values of $\left(\beta C_{L_\alpha}\right)_W$ can be obtained from the charts of Lapin in reference 15 or those of Lagerstrom and Wall in reference 16.

For the purpose of illustrating the behavior of K_B and comparing equations (13) and (15) with slender-body $K_B(s)$, figure 4 has been used together with reference 15 to obtain figure 5, which presents K_B as a function of βA and r/s_m for $\lambda = 0$, 1/2, and 1 and for no trailing-edge sweep. The case of $\lambda = 0$ corresponds to triangular wings (fig. 5(a)), $\lambda = 1$ to rectangular wings (fig. 5(b)), and $\lambda = 1/2$ to trapezoidal wings (fig. 5(c)). For triangular wings, the curve of K_B by the present theory for $\beta A = 0$ is slightly greater than $K_B(s)$ as given by slender-body theory, and has not been included in the figures. For such small values of βA slender-body theory is the more valid. Incidentally, the restriction of equation (11) is met by all triangular wings with no trailing-edge sweep. An examination of figure 5(b) for rectangular wings shows good agreement between slender-body theory and the present theory at $\beta A = 2$, the lowest aspect ratio for which the present theory is applicable to rectangular wings. In the case of the trapezoidal wings (fig. 5(c)), the restriction of equation (11) imposes the condition that $\beta A \geq 4/3$. For a value of βA of 4/3 there is no appreciable difference between slender-body $K_B(s)$ and the value of K_B by the present theory.

On the basis of figures 5(a), 5(b), and 5(c), the following selection rule is given: If $\beta A (1+\lambda)\left(\dfrac{1}{m\beta} + 1\right) < 4$, use the slender-body theory $K_B(s)$; and if $\beta A (1+\lambda)\left(\dfrac{1}{m\beta} + 1\right) > 4$, use K_B. However, for certain combinations of taper and low aspect ratio it may turn out that $K_B > K_B(s)$. In such cases, use $K_B(s)$ since it is more accurate than K_B for small aspect ratios. Although this rule has been derived by comparison between the present theory and slender-body theory for unswept trailing edges, it has also proved valid experimentally for swept-forward trailing edges.

Since rectangular and triangular wings are very common, and since $\left(\beta C_{L_\alpha}\right)_W$ is known in closed form for these plan forms, specialized results can readily be obtained from equations (13) and (15) for K_B. For rectangular wing-body combinations, K_B is given as

$$K_B = \frac{2}{\pi} \frac{1}{\left(\beta A - \frac{1}{2}\right)} \left\{ \frac{1}{2} \left[1 + \frac{\beta A \frac{r}{s_m}}{1 - \frac{r}{s_m}} \right]^2 \cos^{-1} \left[1 + \frac{\frac{1}{\left(1 - \frac{r}{s_m}\right)}}{\beta A \frac{r}{s_m}} \right] - \right.$$

$$\left. \frac{1}{2} \left[\frac{\beta A \frac{r}{s_m}}{1 - \frac{r}{s_m}} \right]^2 \cosh^{-1} \left[1 + \frac{1 - \frac{r}{s_m}}{\beta A \frac{r}{s_m}} \right] - \frac{1}{2} - \frac{\pi}{4} + \frac{1}{2} \sqrt{1 + \frac{2\beta A \frac{r}{s_m}}{1 - \frac{r}{s_m}}} \right\} \quad (16)$$

For triangular wing-body combinations with subsonic leading edges, K_B is given as

$$K_B = \frac{8E\left(\sqrt{1 - \frac{\beta^2 A^2}{4}}\right)}{\pi^2 \left(\frac{\beta A}{4}\right)^2} \left\{ \frac{\left(\frac{\beta A}{4}\right)^2}{2\left(\frac{\beta A}{4} + 1\right)^2} \left[1 + \frac{2\left(1 + \frac{\beta A}{4}\right)\frac{r}{s_m}}{1 - \frac{r}{s_m}} \right]^{3/2} - \left(\frac{\beta A}{\beta A + 4}\right)^2 + \right.$$

$$\left. \frac{\left(\frac{\beta A}{4}\right)^2}{2\left(\frac{\beta A}{4} + 1\right)^2} \left[1 + \frac{2\left(1 + \frac{\beta A}{4}\right)\frac{r}{s_m}}{1 - \frac{r}{s_m}} \right]^{1/2} - 2\left(\frac{\beta A}{4}\right)^2 \left(\frac{\frac{r}{s_m}}{1 - \frac{r}{s_m}}\right)^2 \tanh^{-1} \sqrt{1 + 2\frac{\left(1 + \frac{\beta A}{4}\right)\frac{r}{s_m}}{\left(1 - \frac{r}{s_m}\right)}} \right\}$$

$$(17)$$

and for supersonic leading edges as

$$
K_B = \frac{1}{\pi\sqrt{\left(\frac{\beta A}{4}\right)^2 - 1}} \left\{ \left(\frac{\beta A}{\beta A + 4}\right)\left[1 + \frac{2\left(1+\frac{\beta A}{4}\right)\frac{r}{s_m}}{1 - \frac{r}{s_m}}\right]^2 \cos^{-1}\left[\frac{1 + \frac{\frac{\beta A}{2}\left(1+\frac{\beta A}{4}\right)\frac{r}{s_m}}{1 - \frac{r}{s_m}}}{\frac{\beta A}{4} + \frac{\left(1+\frac{\beta A}{4}\right)\frac{\beta A}{2}\left(\frac{r}{s_m}\right)}{1 - \frac{r}{s_m}}}\right] + \right.
$$

$$
\frac{\sqrt{\left(\frac{\beta A}{4}\right)^2 - 1}}{\left(1 + \frac{\beta A}{4}\right)}\sqrt{-1 + \frac{\beta A \frac{r}{s_m}}{1 - \frac{r}{s_m}}} - \frac{\frac{\beta A}{4}}{1 + \frac{\beta A}{4}}\cos^{-1}\frac{4}{\beta A} -
$$

$$
\sqrt{\left(\frac{\beta A}{4}\right)^2 - 1}\,\beta A\,\frac{\left(\frac{r}{s_m}\right)^2}{\left(1 - \frac{r}{s_m}\right)^2}\cosh^{-1}\left[1 + \frac{2\left(1 - \frac{r}{s_m}\right)}{\beta A \frac{r}{s_m}}\right] - \left. \frac{\sqrt{\left(\frac{\beta A}{4}\right)^2 - 1}}{\left(\frac{\beta A}{4} + 1\right)} \right\}
$$

$$\tag{18}$$

Numerical Example

To illustrate the use of the method developed in the foregoing sections, the determination of the lift-curve slope for a trapezoidal wing-body combination is now presented. Given that $c_t = 1.500$, $c_r = 3.878$, $r = 0.850$, $s_m = 3.790$, $M = 2.87$, and no midchord sweep, the following values of the parameters are obtained:

$$A = \frac{4(2.940)}{1.5 + 3.878} = 2.19, \text{ aspect ratio of wing alone}$$

$$\beta = \sqrt{M^2 - 1} = \sqrt{2.87^2 - 1} = 2.69$$

$$\beta A = 5.89, \text{ effective aspect ratio}$$

$$r/s_m = 0.224, \text{ body-radius, semispan ratio}$$

$$\lambda = \frac{1.500}{3.878} = 0.387, \text{ taper ratio}$$

$$m = \frac{2(2.94)}{(3.878 - 1.5)} = 2.47$$

$$m\beta = 6.64$$

$$\beta d/c_r = \frac{(2.69)(1.7)}{3.878} = 1.18$$

The value of the parameter in equation (11) is

$$\beta A \ (1+\lambda) \left(\frac{1}{m\beta} + 1 \right) = (5.89) \ (1.387) \left(\frac{1}{6.64} + 1 \right) > 4$$

The value of $K_W(s)$ from equation (7) or figure 1 is

$$K_W(s) = 1.18$$

Now determine $K_B(s)$ from figure 1:

$$K_B(s) = 0.31$$

The value of K_B from figure 4 in parametric form is

$$K_B \left(\beta C_{L_\alpha} \right)_W (1+\lambda) \left(\frac{s_m}{r} - 1 \right) = 4.41$$

and the $\left(\beta C_{L_\alpha} \right)_W$ from the charts of reference 16 is

$$\left(\beta C_{L_\alpha} \right)_W = 3.85$$

The value of K_B is thus

$$K_B = \frac{4.41}{(3.85)(1.387)(3.46)} = 0.24$$

Since $K_B < K_B^{(s)}$, the value of K_B is to be used.

$$K = K_W^{(s)} + K_B = 1.18 + 0.24 = 1.42$$

The lift-curve slope of the combination excluding the effect of the nose is thus

$$\left(\beta C_{L_\alpha} \right)_{C-N} = K \left(\beta C_{L_\alpha} \right)_W$$

$$= (1.42)(3.85) = 5.46 \text{ per radian}$$

For the lift-curve slope of the complete combination, the lift due to the nose must be added to $\left(\beta C_{L_\alpha} \right)_{C-N}$. If the nose is slender so that slender-body theory is valid, then

$$\left(\beta C_{L_\alpha} \right)_N = \frac{2\beta \pi r^2}{S}$$

$$= \frac{2(2.69)(\pi)(0.85)^2}{(2.94)(1.500 + 3.878)} = 0.77 \text{ per radian}$$

Finally, the lift-curve slope for the entire configuration is given by

$$\left(\beta C_{L_\alpha} \right)_C = 5.46 + 0.77 = 6.23 \text{ per radian}$$

EXPERIMENTAL VERIFICATION

The results of the foregoing analysis have been applied to the calculation of the lift-curve slopes of nearly 100 wing-body configurations
of widely varying plan forms. The same geometric configuration at two
different Mach numbers has been counted twice. The results are compared
with the experimental lift-curve slopes which were measured in various
wind tunnels. The correlation between the experimental and estimated
results is shown in figures 6, 7, and 8 which apply to triangular, rectangular, and trapezoidal wing-body combinations, respectively. Tables I,
II, and III summarize the geometric and aerodynamic characteristics and
the test conditions for the triangular, rectangular, and trapezoidal
wing-body combinations. A sketch of a wing-body combination defining the
dimensions is given in figure 9, and rough sketches of the combinations
are included in the tables. The sources of the test data are listed in
references 17 to 38; some of the test data are unpublished.

Some difficulty was met in trying to determine lift-curve slope
from published curves since slight nonlinearities near $\alpha = 0$ were present. In the several such cases encountered the curves were essentially
linear for $\pm 2^\circ$, and the average over this range was used. The values of
the lift-curve slope for the bodies alone were in some instances also
difficult to obtain accurately because of the small slopes of the published curves. Furthermore, the reliability of the experimental lift-
curve slopes was sometimes questionable. In one case, data on similar
configurations from different testing facilities (and at different
Reynolds numbers) gave a difference of the order of 10 percent in the
lift-curve slopes. Also, generally speaking, the data have not been
corrected for any flow irregularities that may exist in the various wind
tunnels. In view of these difficulties, together with the approximations
made in the method, it was felt that a correlation of ± 10 percent would
be a realistic accuracy to expect.

The actual lift forces developed by the winged sections of the combinations are not given directly by experiment, so that no direct comparison could be made between the method and experiment for this lift
component. Instead, it was decided to perform the correlation on the
basis of over-all lift-curve slopes of the combinations. The estimated
over-all lift-curve slopes were determined by adding to the contribution
due to the winged part of the combination, as determined by the present
method, the contribution due to the body nose as determined by slender-
body theory. The lift contribution of the nose for combinations having
relatively small wings is large. Consequently, the correlation reflects
in part the ability of slender-body theory to predict the lift of the
nose.

It should be borne in mind that correlation between the method and experiment on the basis of total lift does not necessarily imply that the distribution of lift between body and wing has been correctly predicted by the method. To substantiate this point will require more data on the lift of components than is now available.

Included on the curves of figures 6, 7, and 8 are lines of perfect agreement, and dashed lines indicating ±10-percent deviation from perfect agreement. Data for combinations with no afterbody have been indicated by flagged symbols. It is readily apparent from these figures that the present method estimates the lift-curve slope within ±10 percent for most of the combinations, and thus properly accounts for the first-order effects of wing-body interference.[1] The scatter about the lines of perfect agreement is apparently random and is due to second-order effects that will subsequently be discussed. The points on the correlation curves for configurations with no afterbody have, on the average, higher estimated lift-curve slopes than the experimental, as would be expected since the present method includes afterbody lift.

With regard to triangular wing-body combinations the present method is not substantially different from that of reference 8, which was found to be valid for such combinations. Thus correlation for the triangular wing-body combinations was assured.

For the rectangular wing-body combinations, a point of interest is furnished by the fact that slender-body theory should be inapplicable. Consider the slender-body combination with the area OA'A in figure 10. According to slender-body theory the entire lift is developed on OAA'. If A approaches A', the slender combination becomes nonslender and, on the basis of slender-body theory, the lift remains unchanged and is concentrated on the leading edge of the rectangular half-wing. This application of slender-body theory to rectangular wing-body combinations represents a degenerate case of the theory. It is thus interesting that the use of $K_W(s)$ produces correlation for rectangular wing-body combinations. The good correlation of the trapezoidal wing-body combinations is more significant than that for the triangular or rectangular wing-body combinations because generally four quantities are necessary to describe the geometry of trapezoidal combinations, whereas only two are necessary for the latter combinations.

---

[1]In this connection, it is significant to ask how much error can be introduced by neglecting interference. For the triangular wings of this report it was determined that the sums of the wing-alone and body-alone lift-curve slopes were on the average 20 percent greater than the corresponding experimental lift-curve slopes for the combinations when the wing alone is taken as the triangular wing that includes the blanketed area. For very small wings the sum can approach twice the experimental value.

ADDITIONAL FACTORS AFFECTING LIFT

The scatter that is exhibited by the correlation charts indicates the existence of a number of higher-order effects not fully accounted for by the present method, such as afterbody shape, forebody shape, Reynolds number, angle of attack, and airfoil section.

Afterbody Shape

The length of afterbody behind the wing of a combination has an effect on how much lift is developed by the afterbody. The first few body diameters of afterbody length are the most effective in this respect. Lagerstrom and Graham (reference 39) have studied flat afterbodies behind triangular wings. For the planar case, they find, on the basis of linear theory, that the lift force increases as the afterbody length increases up to a certain optimum length and decreases thereafter. Whether such considerations are also valid in the case of cylindrical afterbodies is not clear. Lagerstrom and Graham imply that theoretically an optimum afterbody length would be expected for the nonplanar case. Data are not yet available to indicate whether an optimum length of afterbody exists for nonplanar combinations when viscosity affects the flow.

Theoretically, boattailing of the afterbody should have the effect of decreasing the lift of the combination if the flow follows the body. Because of separation, it is expected that little, if any, lift will be lost.

Forebody Shape

The forebody shape can influence the lift of a wing-body combination as predicted by the theory of this report in a number of ways. First, if the nose of the combination is not slender, the lift, as predicted by slender-body theory, will be inapplicable. If the wing is located close to the nose, the upwash field will vary chordwise and spanwise instead of only spanwise as assumed in equation (8). The wing of the combination will thus be effectively cambered as well as twisted, and the wing-body interference as well as the lift due to upwash will be altered.

An additional effect of forebody shape is the manner in which it affects the boundary-layer phenomena of the winged part of the combination. For instance, if the same wing were mounted near the base of a

given body rather than near the nose, the boundary layer would be thicker and more serious boundary-layer interference could be anticipated.

Reynolds Number and Angle of Attack

The effect of Reynolds number on the vortex and boundary-layer flows of wing-body combinations is not well understood. While the effects may not be significant for lift at low angles of attack, they are of considerable importance at high angles of attack. In fact, the viscous cross flow of the type discussed by Allen and Perkins in reference 40 is sufficiently important to invalidate at high angles of attack any theory of wing-body combinations based solely on frictionless flow considerations.

Airfoil Section

It is known that the airfoil section can have a large effect on the lift-curve slope of wings of identical plan form. Such an effect is also to be anticipated for combinations in which the wing furnishes most of the lift. It cannot be ascertained without experiment whether the addition of the body will alleviate or aggravate differences in lift-curve slope due to airfoil section since these differences are not yet understood for wings alone.

CONCLUDING REMARKS

On the basis of the correlations between the estimated and experimental lift-curve slopes presented in this report for nearly 100 triangular, rectangular, and trapezoidal wing-body configurations, the leading edges of which are not swept forward and the trailing edges of which are not swept back, it can be concluded that, using the methods of this report, the lift-curve slopes of the combinations can be predicted in most cases within ±10 percent. The scatter observed in the correlation is due to effects such as forebody and afterbody shape, Reynolds number, angle of attack, and airfoil section which cannot be predicted at the present time.

Ames Aeronautical Laboratory,
     National Advisory Committee for Aeronautics,
          Moffett Field, Calif.

REFERENCES

1. Ferrari, Carlo: Interference Between Wing and Body at Supersonic Speeds - Theory and Numerical Application. Jour. Aero. Sci., vol. 15, no. 6, 1948, pp. 317-336.

2. Nielsen, Jack N., and Matteson, Frederick H.: Calculative Method for Estimating the Interference Pressure Field at Zero Lift on a Symmetrical Swept-Back Wing Mounted on a Circular Cylindrical Body. NACA RM A9E19, 1949.

3. Moskowitz, Barry, and Maslen, Stephen H.: Experimental Pressure Distributions Over Two Wing-Body Combinations at Mach Number 1.9. NACA RM E50J09, 1951.

4. Morikawa, George: The Wing-Body Problem for Linearized Supersonic Flow. GALCIT J.P.L. PR 4-116. Dec. 19, 1949.

5. Nielsen, Jack N.: Supersonic Wing-Body Interference. California Institute of Technology, 1951.

6. Stewart, H. J., and Meghreblian, R. V.: Body-Wing Interference in Supersonic Flow. GALCIT J.P.L. PR 4-99, June 2, 1949.

7. Morikawa, George: Supersonic Wing-Body Lift. Jour. Aero. Sci., vol. 18, no. 4, 1951.

8. Nielsen, Jack N., Katzen, Elliott D., and Tang, Kenneth K.: Lift and Pitching-Moment Interference Between a Pointed Cylindrical Body and Triangular Wings of Various Aspect Ratios at Mach Numbers of 1.50 and 2.02. NACA RM A50F06, 1950.

9. Spreiter, John R.: Aerodynamic Properties of Slender Wing-Body Combinations at Subsonic, Transonic, and Supersonic Speeds. NACA Rep. 962, 1948. (Formerly NACA TN's 1662 and 1897)

10. Jones, Robert T.: Properties of Low-Aspect-Ratio Pointed Wings at Speeds Below and Above the Speed of Sound. NACA TN 1032, 1946.

11. Beskin, L.: Determination of Upwash Around a Body of Revolution at Supersonic Velocities. Johns Hopkins Univ. Applied Physics Lab., Rept. No. CM-251, 1946.

12. Lagerstrom, P. A., and Van Dyke, M. D.: General Considerations About Planar and Non-Planar Lifting Systems. Douglas Aircraft Co., Inc., Rept. No. SM-13432, 1949.

13. Jones, Robert T.: Thin Oblique Airfoils at Supersonic Speed.
    NACA Rep. 851, 1946. (Formerly NACA TN 1107)

14. Lagerstrom, P.A.: Linearized Supersonic Theory of Conical Wings.
    NACA TN 1685, 1948.

15. Lapin, Ellis: Charts for the Computation of Lift and Drag of Finite
    Wings at Supersonic Speeds. Douglas Aircraft Co., Inc.,
    Rept. No. SM-13480, 1949.

16. Lagerstrom, P. A., Wall, D., and Graham, M. E.: Formulas in Three-
    Dimensional Wing Theory. Douglas Aircraft Co., Inc.,
    Rept. No. SM-11901, 1946.

17. Spahr, J. Richard, and Robinson, Robert A.: Wind-Tunnel Investiga-
    tion at Mach Numbers of 1.5 and 2.0 of a Canard Missile Configura-
    tion. NACA RM A51C08, 1951.

18. Jevon, R. W.: Data Report for Supersonic Wind Tunnel Tests on
    XSSM-N-6 Models #3C and #6A. Fifth Daingerfield Test Period,
    M = 2.0. Grumman Aircraft Engineering Corp., Rept. No. 3147.20,
    March, 1950.

19. Jevon, R. W., and Bastedo, W. Jr.: Data Report for Supersonic Wind
    Tunnel Tests on XSSM-N-6 Model #3A. First Daingerfield Test
    Period, M = 2.0. Grumman Aircraft Engineering Corp.,
    Rept. No. P/A 3128.20, April 1949.

20. Jevon, R. W.: Data Report for Supersonic Wind Tunnel Tests on
    XSSM-N-6 Models #3B and #4A. 2nd-4th Daingerfield Test Periods,
    M = 2.0, 2.25, 1.73. Grumman Aircraft Engineering Corp.,
    Rept. No. P/A 3141.20, Sept. 1949.

21. Bastedo, W. Jr.: Data Report for Supersonic Wind Tunnel Tests on
    XSSM-N-6 Model #6. 2nd Aberdeen Test Period, M = 1.72.
    Grumman Aircraft Engineering Corp., Rept. No. P/A 3107.21,
    July 1949.

22. Katzen, Elliott D., and Kaattari, George E.: Drag Interference
    Between a Pointed Cylindrical Body and Triangular Wings of Various
    Aspect Ratios at Mach Numbers of 1.50 and 2.02. NACA RM A51C27,
    1951.

23. Peters, R. G.: Data Report for Supersonic Wind Tunnel Tests on
    GAPA Model FR-87. Sixth and Seventh Aberdeen Test Periods,
    M = 1.72 and M = 1.28. Boeing Airplane Co., D-8788,
    (Tech. Rept. No. 111-9), Feb. 1948.

24. Peters, R. G.: Data Report for Supersonic Wind Tunnel Tests on GAPA Model FR-87. Fifth Aberdeen Test Period, M = 1.72. Boeing Aircraft Co., D-8397, (Tech. Rept. No. 111-7), Aug. 1947.

25. Rainey, Robert W.: Langley 9-Inch Supersonic Tunnel Tests of Several Modifications of a Supersonic Missile Having Tandem Cruciform Lifting Surfaces. Three-Component Data Results of Models Having Ratios of Wing Span to Tail Span Equal to 1. NACA RM L9L30, 1951.

26. Rainey, Robert W.: Langley 9-Inch Supersonic Tunnel Tests of Several Modifications of a Supersonic Missile Having Tandem Cruciform Lifting Surfaces. Three-Component Data Results of Models Having Ratios of Wing Span to Tail Span Less Than 1. NACA RM L50I29a, 1950.

27. Rainey, Robert W.: Langley 9-Inch Supersonic Tunnel Tests of Several Modifications of a Supersonic Missile Having Tandem Cruciform Lifting Surfaces. Three-Component Data Results of Models Having Ratios of Wing Span to Tail Span Equal to and Less Than 1 and Some Static Rolling-Moment Data. NACA RM L50G07, 1951.

28. Speth, Robert F.: Results of Rascal Supersonic Wind Tunnel Tests at M = 1.72. Bell Aircraft Corp., Rept. No. 56-980-001, vol. 1, Dec. 1948.

29. Speth, Robert F.: Results of Rascal Supersonic Wind Tunnel Tests at M = 1.28. Bell Aircraft Corp., Rept. No. 56-980-001, vol. 2, Dec. 1948.

30. Harshman, J. D., and Uddenberg, R. C.: Supersonic Wind Tunnel Tests of GAPA Models at a Mach Number of 1.28 in the Aberdeen Tunnel. Boeing Aircraft Co., Rept. D-7817, Aug. 2, 1946.

31. Uddenberg, R. C.: Supersonic Wind Tunnel Tests of GAPA Models at a Mach Number of 1.72 in the Aberdeen Tunnel. Boeing Aircraft Co., Rept. D-7818, Dec. 1946.

32. Flake, H. M.: Supersonic Wind Tunnel Tests of a 0.020-Scale Model of the NA-705 Missile at Mach Number 2.87 to Determine Effect of Aspect Ratio and Planform of Wings on the Aerodynamic Characteristics of Wing Plus Body. North American Aviation, Inc., Rept. No. AL-1156, Oct. 1950.

33. Hall, Albert W., and Morris, Garland J.: Aerodynamic Characteristics at a Mach Number of 1.25 of a 6-Percent-Thick Triangular Wing and 6- and 9-Percent-Thick Triangular Wings in Combination With a Fuselage-Wing Aspect Ratio 2.31, Biconvex Airfoil Sections. NACA RM L50D05, 1950.

34. Fischer, H. S.: Supersonic Wind-Tunnel Tests of a 0.075-Scale
       Model of the Nike 482 Missile. Douglas Aircraft Co., Inc.,
       Rept. No. SM-13848, Nov. 1950.

35. Grigsby, Carl E.: Investigation at a Mach Number of 1.93 to Deter-
       mine Lift, Drag, Pitching Moment, and Average Downwash Character-
       istics for Several Missile Configurations Having Rectangular Wings
       and Tails of Various Spans. NACA RM L50I08, 1950.

36. Ellis, Macon C., Jr., and Grigsby, Carl E.: Aerodynamic Investiga-
       tion at Mach Number 1.92 of a Rectangular Wing and Tail and Body
       Configuration and Its Components. NACA RM L9L28a, 1950.

37. Jaeger, B. F., and Brown, A. E.: The Aerodynamic Characteristics at
       Mach Number 2.0 of 14- and 18-Caliber Fin-Stabilized Rockets With
       Varying Body and Fin Parameters. U. S. Naval Ordnance Test
       Station, Inyokern, Calif., NAVORD Rept. 1211, Jan. 1950.

38. Dorrance, W. H.: Body-Tail Interference in Supersonic Flow Includ-
       ing an Example Application. University of Michigan, UMM-38,
       Aug. 1949.

39. Lagerstrom, P. A., and Graham, M. E.: Aerodynamic Interference in
       Supersonic Missiles. Douglas Aircraft Co., Inc.,
       Rept. No. SM-13743, 1950.

40. Allen, H. Julian, and Perkins, Edward W.: Characteristics of Flow
       Over Inclined Bodies of Revolution. NACA RM A50L07, 1951.

TABLE I.- SUMMARY OF AERODYNAMIC AND GEOMETRIC CHARACTERISTICS AND TEST CONDITIONS FOR TRIANGULAR WING BODY-COMBINATIONS

No.	Sketch	M_0	R	Wing section	$\bar{c}$ (in.)	βA	$\Lambda_{L.E.}$ (deg)	$\frac{r}{b_m}$	$\frac{l_a}{r}$	$\frac{l_f}{r}$	Reference	Facility
1		1.5	1.0×10^6	[1]d.w.	2	0.75	80.4	0.600	4	6.7	8	Ames 1×3 ft
2		2.0	1.0×10^6	d.w.	2	1.16	80.4	.600	4	6.7	8	Ames 1×3 ft
3		1.5	1.0×10^6	d.w.	2	1.50	71.6	.428	4	6.7	8	Ames 1×3 ft
4		2.0	1.0×10^6	d.w.	2	2.32	71.6	.428	4	6.7	8	Ames 1×3 ft
5		1.5	1.0×10^6	d.w.	2	2.26	63.2	.333	4	6.7	8	Ames 1×3 ft
6		2.0	1.0×10^6	d.w.	2	3.50	63.2	.333	4	6.7	8	Ames 1×3 ft
7		1.5	1.0×10^6	d.w.	2	3.01	56.0	.272	4	6.7	8	Ames 1×3 ft
8		2.0	1.0×10^6	d.w.	2	4.66	56.0	.272	4	6.7	8	Ames 1×3 ft
9		1.5	1.0×10^6	d.w.	2	3.72	50.3	.231	4	6.7	8	Ames 1×3 ft
10		2.0	1.0×10^6	d.w.	2	5.77	50.3	.231	4	6.7	8	Ames 1×3 ft
11		1.5	1.0×10^6	d.w.	2	4.47	45.0	.201	4	6.7	8	Ames 1×3 ft
12		2.0	1.0×10^6	d.w.	2	6.93	45.0	.201	4	6.7	8	Ames 1×3 ft
13		1.72	1.24×10^6	d.w.	3	1.50	75	.272	8.2	24.2	34	Aberdeen
14		1.25	$.88\times10^6$	[2]b.c.	3.51	1.73	60	.163	6.1	9.1	33	Langley 9 in.
15		1.28	1.11×10^6	d.w.	2.57	1.89	59.4	.215	7.7	10.1	30	Aberdeen
16		1.72	1.11×10^6	d.w.	2.57	3.31	59.4	.215	7.7	10.1	31	Aberdeen
17		2.87	$.56\times10^6$	d.w.	2.65	10.76	45	.176	5.5	18.0	32	NAA 16 in.
18		2.87	$.56\times10^6$	d.w.	2.65	10.76	0	.176	3.9	19.6	32	NAA 16 in.
19		2.87	$.74\times10^6$	d.w.	3.49	6.20	60	.220	5.0	17.1	32	NAA 16 in.
20		2.87	$.74\times10^6$	d.w.	3.49	6.20	0	.220	3.0	19.1	32	NAA 16 in.
21		2.87	1.11×10^6	d.w.	5.12	2.88	75	.292	4.1	15.2	32	NAA 16 in.
22		2.87	1.11×10^6	d.w.	5.12	2.88	0	.292	1.0	18.2	32	NAA 16 in.
23		1.15	1.26×10^6	d.w.	7.54	1.31	60	.216	13.9	11.6		Ames 6×6 ft
24		1.2	1.26×10^6	d.w.	7.54	1.53	60	.216	13.9	11.6		Ames 6×6 ft
25		1.3	1.26×10^6	d.w.	7.54	1.92	60	.216	13.9	11.6		Ames 6×6 ft
26		1.4	1.26×10^6	d.w.	7.54	2.26	60	.216	13.9	11.6		Ames 6×6 ft
27		1.53	1.26×10^6	d.w.	7.54	2.68	60	.216	13.9	11.6		Ames 6×6 ft
28		1.7	1.26×10^6	d.w.	7.54	3.18	60	.216	13.9	11.6		Ames 6×6 ft
29		1.2	$.59\times10^6$	d.w.	3.53	2.66	45	.254	0	28.9		Ames 6×6 ft
30		1.4	$.59\times10^6$	d.w.	3.53	3.92	45	.254	0	28.9		Ames 6×6 ft
31		1.7	$.59\times10^6$	d.w.	3.53	5.50	45	.254	0	28.9		Ames 6×6 ft
32		1.93	$.20\times10^6$	[3]hex.	.65	3.81	60	.382	12.1	10.1		Langley 9 in.
33		1.62	$.23\times10^6$	hex.	.65	2.94	60	.382	12.1	10.1		Langley 9 in.

[1]d.w. indicates double wedge.
[2]b.c. indicates biconvex.
[3]hex. indicates hexagonal.

NACA

TABLE I.- CONCLUDED

No.	$\beta A(1+\lambda)\left(\frac{1}{m\beta}+1\right)$	K_B	K_W (s)	Theoretical $\beta\left(C_{L_\alpha}\right)_W$	$\beta\left(C_{L_\alpha}\right)_N$	$\beta\left(C_{L_\alpha}\right)_C$	Experimental $\beta\left(C_{L_\alpha}\right)_B$	$\beta\left(C_{L_\alpha}\right)_C$
1	4.7	0.97	1.56	1.13	2.63	5.48	2.56	6.35
2	5.1	.94	1.56	1.67	4.08	8.25	5.38	10.02
3	5.5	.60	1.38	2.07	1.32	5.41	1.29	5.86
4	6.3	.52	1.38	2.88	2.04	7.52	2.69	8.33
5	6.3	.41	1.29	2.83	.88	5.69	.86	5.77
6	7.5	.37	1.29	3.73	1.36	7.54	1.79	8.24
7	7.0	.32	1.23	3.42	.66	5.95	.64	5.71
8	8.7	.30	1.23	4.00	1.02	7.14	1.35	7.76
9	7.7	.26	1.19	3.86	.53	6.13	.52	5.69
10	9.8	.26	1.19	4.00	.82	6.62	1.08	7.55
11	8.5	.23	1.16	4.00	.44	6.01	.43	5.69
12	10.9	.23	1.16	4.00	.68	6.24	.90	7.09
13	5.5	.34	1.23	2.08	.33	3.59	--	3.63
14	5.7	.20	1.17	2.33	.11	3.29	--	3.09
15	5.9	.25	1.18	2.49	.22	3.78	.28	3.62
16	7.3	.24	1.18	3.61	.39	5.50	.47	5.05
17	14.8	.20	1.14	4.00	.77	6.14	.91	6.74
18	10.8	.25	1.14	4.00	.77	6.32	.91	6.55
19	10.2	.22	1.18	4.00	.77	6.37	.91	6.94
20	6.2	.31	1.18	4.00	.77	6.73	.91	6.60
21	6.9	.33	1.25	3.33	.77	6.04	.91	5.77
22	2.9	.43	1.25	3.33	.77	6.35	.91	5.47
23	5.3	.27	1.18	1.86	.16	2.84	--	3.01
24	5.5	.26	1.18	2.11	.18	3.22	--	3.39
25	5.9	.25	1.18	2.51	.23	3.83	--	3.95
26	6.3	.25	1.18	2.83	.27	4.31	--	4.41
27	6.7	.25	1.18	3.17	.32	4.84	--	4.88
28	7.2	.24	1.18	3.53	.38	5.38	--	5.36
29	6.7	.29	1.21	3.10	.48	5.13	--	4.91
30	7.9	.27	1.21	3.96	.71	6.58	--	6.21
31	9.5	.29	1.21	4.00	1.00	7.00	--	7.26
32	7.8	.42	1.33	3.92	2.29	9.15	2.48	8.93
33	6.9	.44	1.33	3.39	1.77	7.77	1.72	7.66

TABLE II.- SUMMARY OF AERODYNAMIC AND GEOMETRIC CHARACTERISTICS
AND TEST CONDITIONS FOR RECTANGULAR WING-BODY COMBINATIONS

No.	Sketch	M_b	R	Wing Section	$\bar{c}$ (in.)	βA	$\dfrac{r}{a_m}$	$\dfrac{l_a}{r}$	$\dfrac{l_f}{r}$	Reference	Facility
1		1.93	0.19×10^6	[1]b.c.	0.59	9.41	0.172	12.4	11.0	35	Langley 9 in.
2		1.93	$.19 \times 10^6$	b.c.	.59	7.35	.210	12.4	11.0	35	Langley 9 in.
3		1.93	$.19 \times 10^6$	b.c.	.59	5.24	.273	12.4	11.0	35	Langley 9 in.
4		1.93	$.19 \times 10^6$	b.c.	.59	3.16	.382	12.4	11.0	35	Langley 9 in.
5		1.92	$.40 \times 10^6$	b.c.	1.25	5.64	.140	11.2	10.2	36	Langley 9 in.
6		1.28	$.56 \times 10^6$	[2]hex.	1.30	4.27	.153	8.8	13.1	30	Aberdeen
7		1.28	1.12×10^6	hex.	2.60	1.07	.265	7.6	12.2	30	Aberdeen
8		1.72	1.12×10^6	hex.	2.60	1.87	.265	7.6	12.2	31	Aberdeen
9		1.72	$.56 \times 10^6$	hex.	1.30	7.48	.153	8.8	13.1	31	Aberdeen
10		1.72	$.66 \times 10^6$	hex.	1.54	1.87	.379	0.0	21.5	31	Aberdeen
11		1.62	$.40 \times 10^6$	- - -	1.25	1.66	.350	6.8	9.8		Langley 9 in.
12		1.93	$.40 \times 10^6$	- - -	1.25	2.14	.350	6.8	9.8		Langley 9 in.
13		2.40	$.40 \times 10^6$	- - -	1.25	2.84	.350	6.8	9.8		Langley 9 in.
14		1.90	$.50 \times 10^6$	[3]d.w.	1.47	1.86	.384	0.0	14.5	38	Mich. U.
15		2.00	$.79 \times 10^6$	d.w.	3.00	4.76	.083	.4.0	10.9		Ames 1x3 ft
16		1.50	$.91 \times 10^6$	d.w.	3.00	3.08	.083	4.0	10.9		Ames 1x3 ft
17		1.93	$.18 \times 10^6$	b.c.	.59	3.17	.382	12.4	11.0		Langley 9 in.
18		1.62	$.21 \times 10^6$	b.c.	.59	2.45	.382	12.4	11.0		Langley 9 in.
19		2.00	- - -	- - -	1.32	1.73	.333	0.0	24.0	37	Dainger-field
20		2.00	- - -	- - -	1.32	3.46	.200	0.0	24.0	37	Dainger-field

[1]b.c. indicates biconvex
[2]hex. indicates hexagonal
[3]d.w. indicates double wedge

NACA

TABLE II.- CONCLUDED

No.	$\beta A(1+\lambda)\left(\frac{1}{m\beta}+1\right)$	K_B	K_W (s)	Theoretical			Experimental	
				$\beta\left(C_{L_\alpha}\right)_W$	$\beta\left(C_{L_\alpha}\right)_N$	$\beta\left(C_{L_\alpha}\right)_C$	$\beta\left(C_{L_\alpha}\right)_B$	$\beta\left(C_{L_\alpha}\right)_C$
1	18.8	0.12	1.14	3.79	.64	5.40	0.64	5.44
2	14.7	.16	1.17	3.73	.82	5.76	.82	5.47
3	10.5	.22	1.23	3.62	1.15	6.41	1.15	6.69
4	6.3	.40	1.33	3.37	1.90	7.73	1.90	7.16
5	11.3	.12	1.11	3.65	.23	4.71	.23	4.37
6	8.5	.14	1.12	3.53	.22	4.67	.19	5.08
7	2.1	.38	1.22	2.13	.22	3.63	.19	3.46
8	3.7	.38	1.22	2.93	.38	5.07	.40	4.70
9	15.0	.12	1.12	3.73	.38	5.00	.40	5.36
10	3.7	.58	1.33	2.93	1.09	6.68	1.14	6.38
11	3.3	.52	1.30	2.79	.76	5.84	.80	4.71
12	4.3	.44	1.30	3.07	.98	6.32	1.05	5.66
13	5.7	.38	1.30	3.30	1.29	6.84	1.34	6.72
14	3.7	.59	1.33	2.92	1.13	6.74	1.48	6.51
15	9.5	.08	1.06	3.58	.06	4.14	--	4.11
16	6.2	.09	1.06	3.35	.04	3.89	--	4.05
17	6.3	.40	1.33	3.37	1.90	7.73	2.04	7.93
18	4.9	.45	1.33	3.18	1.47	7.13	1.53	6.97
19	3.5	.50	1.28	2.84	.68	5.73	.68	5.48
20	6.9	.20	1.16	3.42	.34	4.98	.34	4.88

NACA

TABLE III.– SUMMARY OF AERODYNAMIC AND GEOMETRIC CHARACTERISTICS AND
TEST CONDITIONS FOR TRAPEZOIDAL WING–BODY COMBINATIONS

No.	Sketch	M_o	R	Wing Section	$\bar{c}$ (in.)	A	λ	$\Lambda_{L.E.}$ (deg)	$\frac{r}{b_2}$	$\frac{l_a}{r}$	$\frac{l_f}{r}$	Reference	Facility
1		1.5	0.26×10^6	[1] d.w.	0.39	2.98	0.500	26.6	0.486	18.5	3.4	17	Ames 1x3 ft
2		2.0	$.26\times10^6$	d.w.	.39	4.62	.500	26.6	.486	18.5	3.4	17	Ames 1x3 ft
3		1.5	$.70\times10^6$	[2] hex.	1.06	3.30	.461	14.0	.250	5.9	14.5	17	Ames 1x3 ft
4		2.0	$.70\times10^6$	hex.	1.06	5.11	.461	14.0	.250	5.9	14.5	17	Ames 1x3 ft
5		1.5	$.56\times10^6$	hex.	.85	2.98	.500	20.5	.314	6.0	14.8	17	Ames 1x3 ft
6		2.0	$.56\times10^6$	hex.	.85	4.61	.500	20.5	.314	6.0	14.8	17	Ames 1x3 ft
7		2.0	$.46\times10^6$	d.w.	.77	4.62	.500	26.6	.486	18.5	3.4	19	Dainger-field
8		1.73	$.42\times10^6$	d.w.	.77	3.77	.500	26.6	.486	18.5	3.4	20	Dainger-field
9		2.25	$.52\times10^6$	d.w.	.77	5.38	.500	26.6	.486	18.5	3.4	20	Dainger-field
10		1.72	– – –	hex.	1.13	3.73	.500	20.5	.314	6.0	14.8	21	Aberdeen
11		1.73	$.92\times10^6$	hex.	1.70	3.77	.500	20.5	.314	6.0	14.8	20	Dainger-field
12		2.0	1.27×10^6	hex.	2.12	5.11	.461	14.0	.250	5.9	14.5	19	Dainger-field
13		2.0	1.02×10^6	hex.	1.70	4.61	.500	20.5	.314	6.0	14.8	18	Dainger-field
14		2.25	1.14×10^6	hex.	1.70	5.37	.500	20.5	.314	6.0	14.8	20	Dainger-field
15		1.96	2.03×10^6	d.w.	3.90	2.09	.302	60	.465	0	4.2		Langley 9 in.
16		1.28	1.05×10^6	hex.	2.49	1.07	.130	60	.265	9.9	6.7	23	Aberdeen
17		1.72	1.05×10^6	hex.	2.49	1.87	.130	60	.265	4.1	12.6	24	Aberdeen
18		1.28	$.80\times10^6$	hex.	1.90	1.60	.253	50	.228	11.2	7.4	23	Aberdeen
19		1.72	$.80\times10^6$	hex.	1.90	2.80	.253	50	.228	11.2	7.4	24	Aberdeen
20		1.93	$.27\times10^6$	hex.	.85	2.03	.305	60	.465	0	17.1	25	Langley 9 in.
21		2.40	$.47\times10^6$	hex.	1.79	2.11	.203	70	.356	0	16.6	26	Langley 9 in.
22		1.93	$.58\times10^6$	hex.	1.79	1.59	.203	70	.356	0	16.6	26	Langley 9 in.
23		1.72	$.80\times10^6$	hex.	1.90	2.80	.253	50	.228	4.4	14.2	24	Aberdeen
24		1.62	$.31\times10^6$	hex.	.85	1.57	.305	60	.465	0	19.0	27	Langley 9 in.
25		1.93	$.28\times10^6$	hex.	.85	2.03	.305	60	.465	0	19.0	27	Langley 9 in.
26		1.93	$.33\times10^6$	hex.	1.02	1.69	.323	15	.465	7.8	10.6	27	Langley 9 in.
27		1.93	$.24\times10^6$	hex.	.74	3.16	.352	45	.388	0	20.4	27	Langley 9 in.
28		1.93	$.83\times10^6$	hex.	2.57	1.05	.400	70	.356	0	14.5	27	Langley 9 in.
29		1.72	$.78\times10^6$	d.w.	1.86	3.75	.333	29.2	.228	.8	19.6	28	Aberdeen
30		1.28	$.46\times10^6$	d.w.	1.16	2.14	.333	29.2	.228	.8	19.6	29	Aberdeen
31		1.72	$.54\times10^6$	d.w.	1.28	3.76	.333	29.2	.300	16.6	5.0	28	Aberdeen
32		1.28	$.34\times10^6$	d.w.	.80	2.15	.333	29.2	.300	16.6	5.0	29	Aberdeen
33		1.28	1.24×10^6	hex.	2.89	1.07	.268	60	.265	7.3	10.1	30	Aberdeen
34		1.72	1.24×10^6	hex.	2.89	1.87	.268	60	.265	7.3	10.1	31	Aberdeen
35		1.28	1.17×10^6	hex.	2.73	1.07	.444	30	.265	6.8	11.4	30	Aberdeen
36		1.72	1.17×10^6	hex.	2.73	1.87	.444	30	.265	6.8	11.4	31	Aberdeen
37		2.87	$.60\times10^6$	d.w.	2.87	5.89	.387	22	.224	4.8	18.9	32	NAA 16x16 in.
38		2.87	$.79\times10^6$	d.w.	3.75	5.38	0	45	.232	3.8	17.9	32	NAA 16x16 in.
39		2.87	1.04×10^6	d.w.	4.94	3.11	0	60	.284	2.7	16.8	32	NAA 16x16 in.
40		1.93	$.30\times10^6$	hex.	.97	2.57	0	60	.382	10.8	10.1		Langley 9 in.
41		1.62	$.34\times10^6$	hex.	.97	1.99	0	60	.382	10.8	10.1		Langley 9 in.

[1] d.w. indicates double wedge.
[2] hex. indicates hexagonal.

TABLE III.- CONCLUDED

| No.	$\beta A(1+\lambda)\left(\dfrac{1}{m\beta}+1\right)$	K_B	K_W (s)	Theoretical $\beta\left(C_{L_\alpha}\right)_W$	$\beta\left(C_{L_\alpha}\right)_N$	$\beta\left(C_{L_\alpha}\right)_C$	Experimental $\beta\left(C_{L_\alpha}\right)_B$	$\beta\left(C_{L_\alpha}\right)_C$
1	6.5	0.56	1.44	3.49	4.83	11.81	4.98	11.05
2	8.9	.50	1.44	3.73	7.48	14.72	9.20	16.29
3	5.9	.29	1.21	3.56	.57	5.91	.59	6.10
4	8.5	.27	1.21	3.78	.89	6.48	1.09	7.15
5	6.0	.41	1.27	3.50	.98	6.86	1.01	7.15
6	8.4	.32	1.27	3.72	1.51	7.42	1.86	8.20
7	8.9	.50	1.44	3.73	7.48	14.72	7.93	15.42
8	7.7	.52	1.44	3.65	6.09	13.24	6.55	12.21
9	10.1	.48	1.44	3.80	8.70	16.00	9.10	16.95
10	7.1	.34	1.27	3.62	1.22	7.05	1.44	7.19
11	7.2	.33	1.27	3.62	1.23	7.02	1.30	6.71
12	8.5	.26	1.21	3.78	.89	6.45	.94	6.25
13	8.4	.32	1.27	3.72	1.51	7.42	1.60	7.60
14	9.6	.31	1.27	3.77	1.76	7.72	1.85	8.08
15	5.5	.61	1.41	2.95	2.48	8.44	3.20	8.67
16	3.8	.39	1.22	2.04	.22	3.51	.27	3.53
17	4.7	.33	1.22	3.06	.38	5.12	.44	4.18
18	5.0	.26	1.19	2.64	.22	4.05	.27	4.03
19	6.5	.23	1.19	3.68	.38	5.61	.44	5.36
20	5.4	.57	1.41	3.12	2.42	8.60	2.79	8.69
21	5.7	.40	1.31	3.13	1.01	6.37	1.38	6.16
22	5.1	.43	1.31	2.58	.76	5.25	.92	4.87
23	6.5	.23	1.19	3.68	.38	5.61	.44	5.14
24	4.8	.67	1.41	2.62	1.87	7.32	2.15	6.12
25	5.4	.57	1.41	3.12	2.42	8.60	2.91	7.78
26	4.6	.63	1.41	2.94	2.01	8.01	2.41	7.74
27	6.9	.37	1.34	3.67	1.99	8.27	2.39	6.80
28	3.8	.54	1.31	1.94	.49	4.08	.59	3.90
29	7.1	.25	1.19	3.73	.52	5.89	.52	5.71
30	4.9	.28	1.19	3.27	.29	5.10	.30	4.42
31	7.1	.33	1.25	3.73	1.08	6.98	1.12	7.38
32	4.9	.37	1.25	3.27	.62	5.92	.66	5.68
33	4.3	.33	1.22	1.97	.22	3.27	.28	3.21
34	5.3	.30	1.22	2.94	.38	4.85	.46	4.64
35	2.6	.39	1.22	2.06	.22	3.54	.28	3.36
36	3.8	.39	1.22	3.08	.38	5.34	.46	4.77
37	9.4	.24	1.18	3.85	.77	6.23	.91	6.30
38	7.4	.33	1.19	3.85	.77	6.62	.91	6.50
39	5.1	.42	1.24	3.65	.77	6.83	.91	6.50
40	5.3	.52	1.33	3.53	1.54	8.06	1.67	7.69
41	4.7	.54	1.33	3.05	1.19	6.89	1.16	6.50
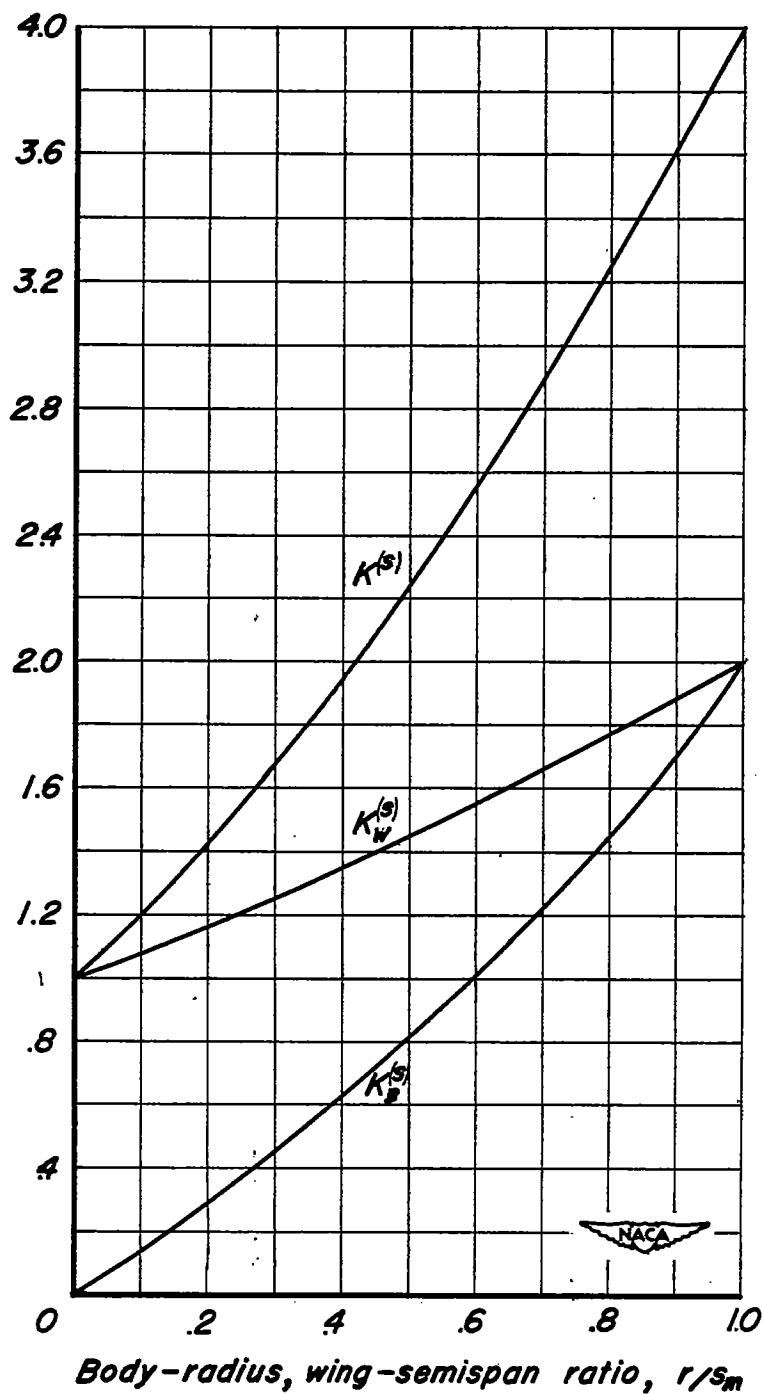
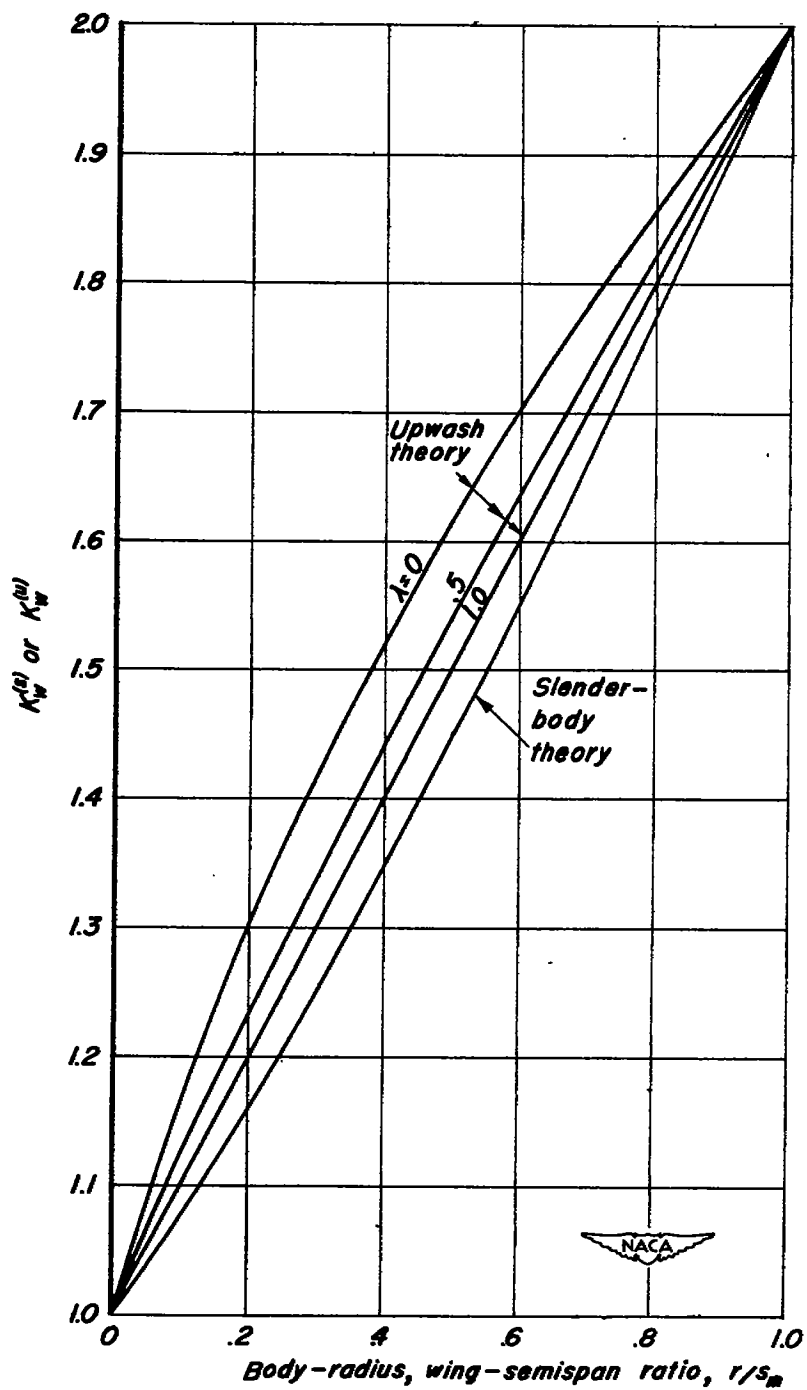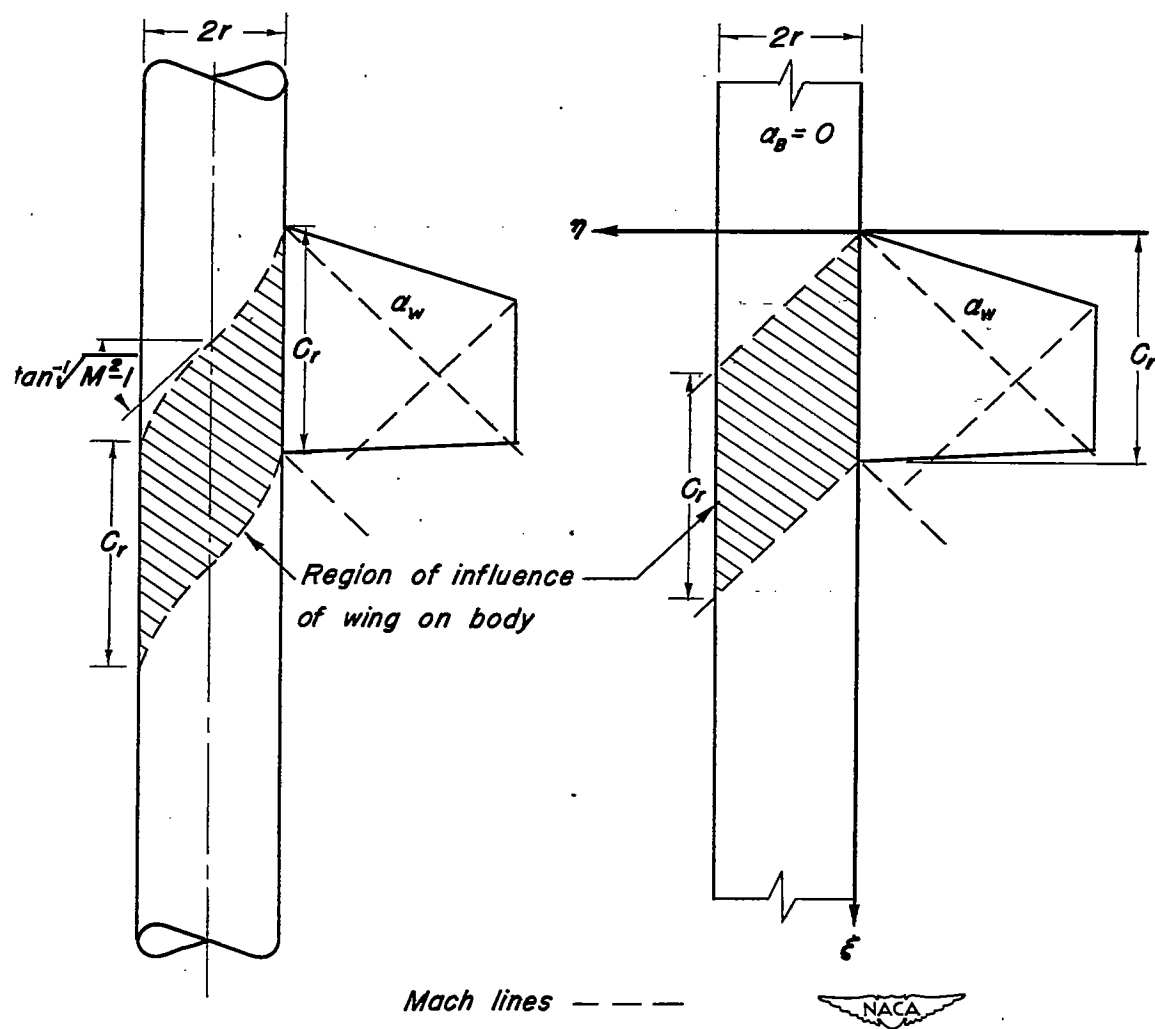Figure I.- Values of $K^{(s)}$, $K_W^{(s)}$, and $K_B^{(s)}$ from slender-body theory.

Figure 2. - Comparison of K_w determined by slender-body and upwash theories.

$tan^{-1}\sqrt{M^2-1}$

a_w

C_r

C_r

Region of influence
of wing on body

$2r$

$a_B = 0$

η

a_w

C_r

C_r

ξ

Region of influence

Mach lines — — —

(a) Nonplanar case.

(b) Equivalent planar case.

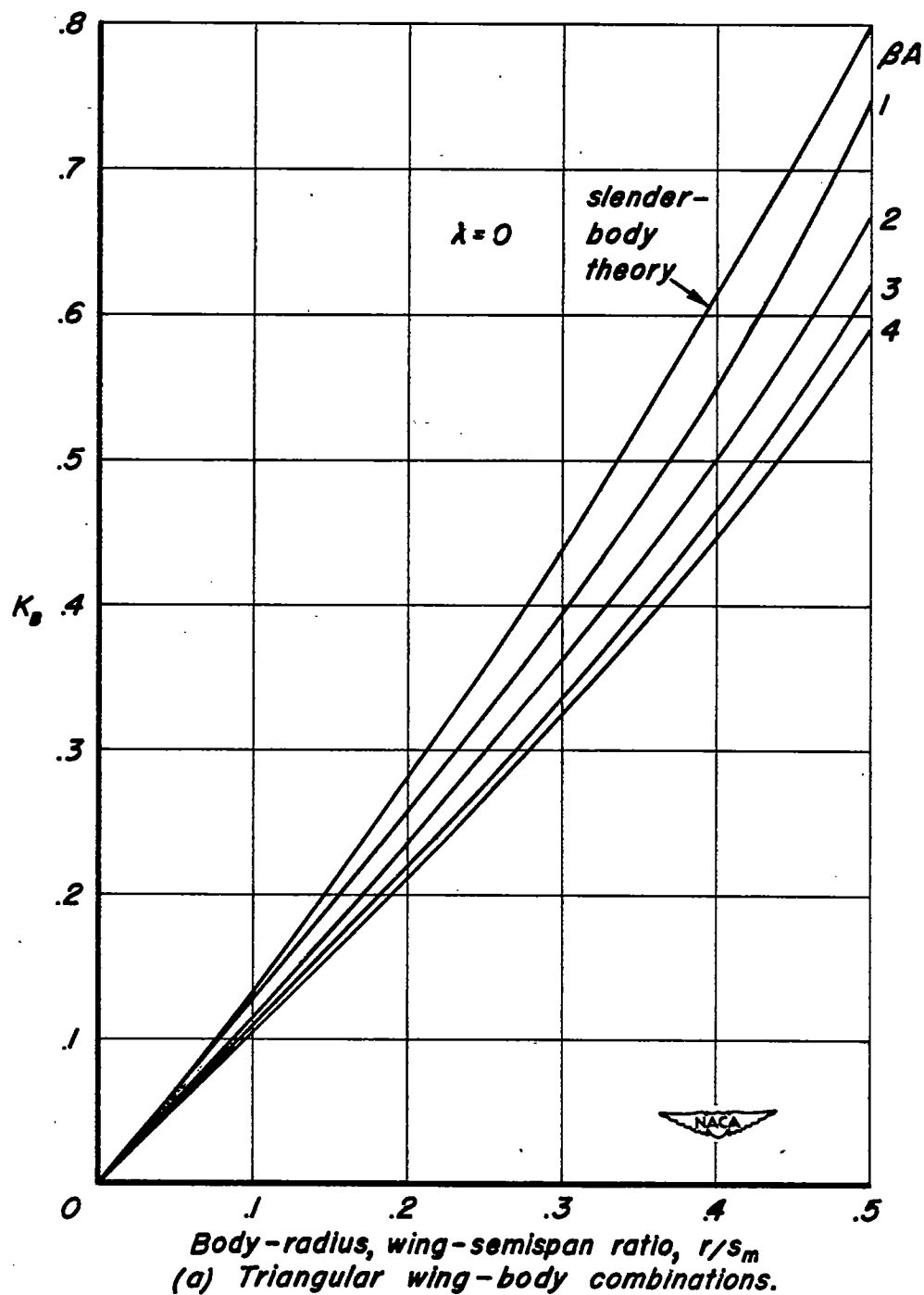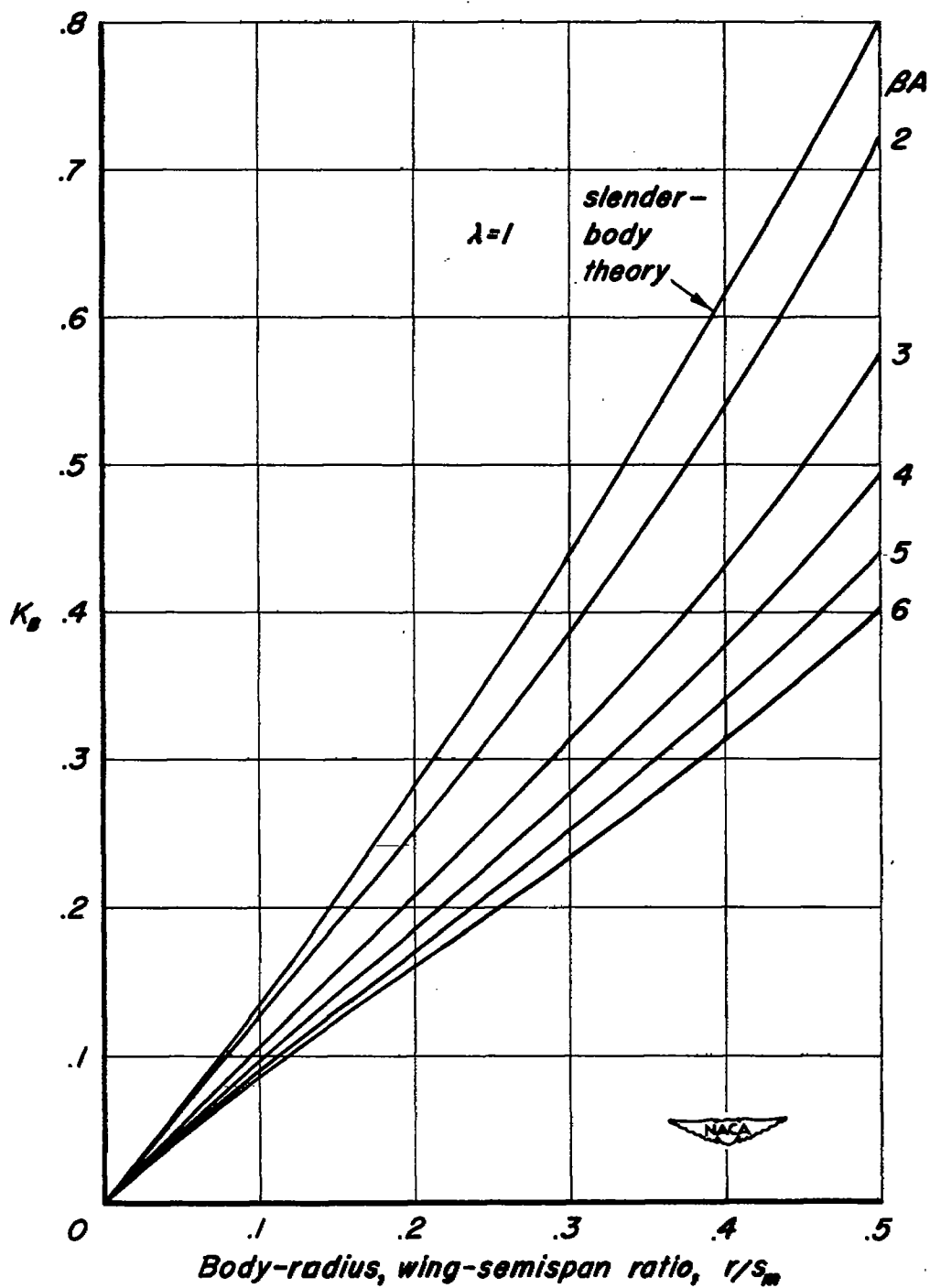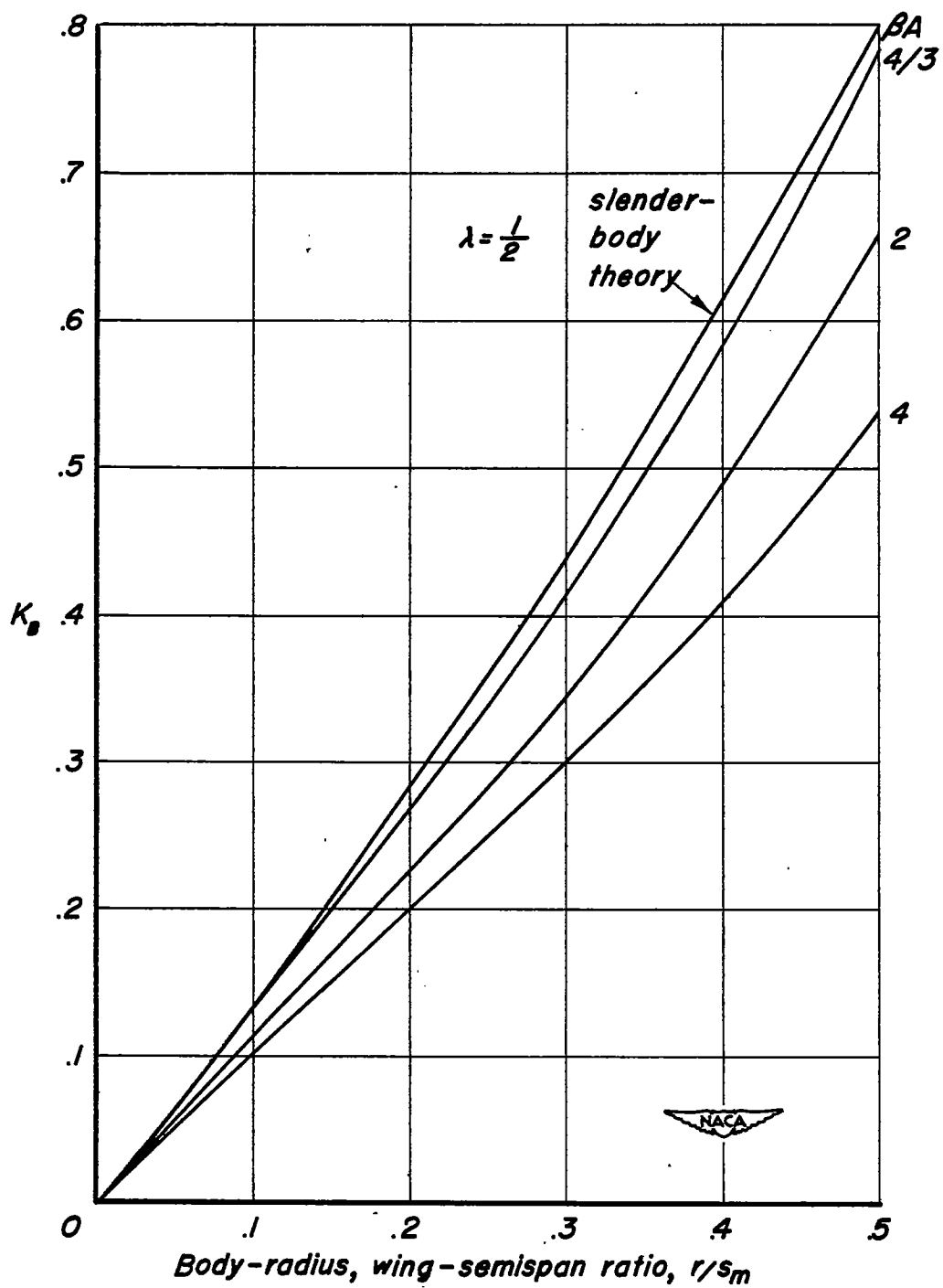Figure 3. — Region of influence of half-wing on body.
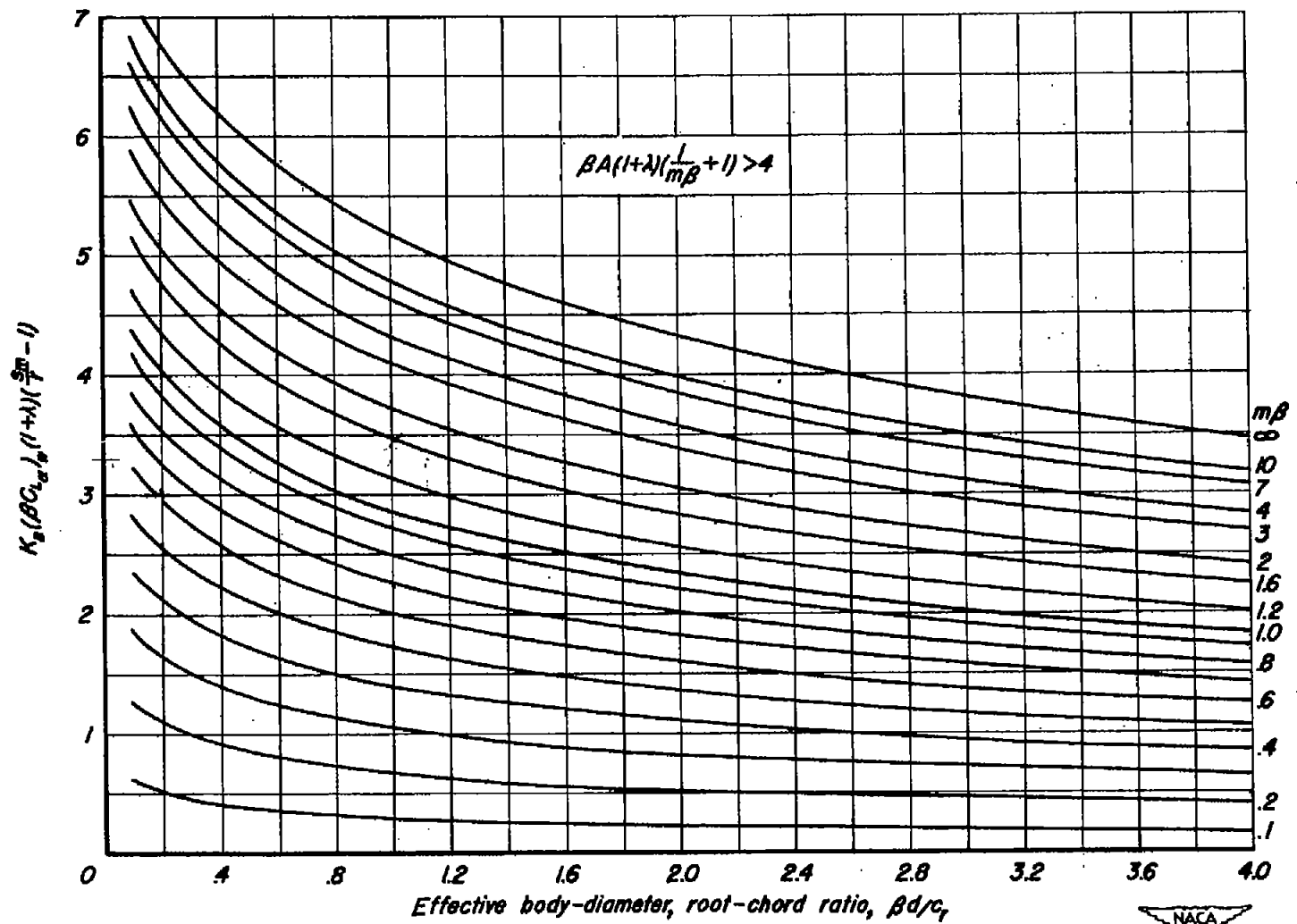
Figure 4.—Design chart for determination of K_B.

Body-radius, wing-semispan ratio, r/s_m

(a) Triangular wing-body combinations.

Figure 5.— Comparison of K_s determined by slender-body theory and present theory for wings with no trailing-edge sweep.

(b) Rectangular wing-body combinations.
Figure 5. – Continued.

(c) Trapezoidal wing-body combinations.

Figure 5. – Concluded.
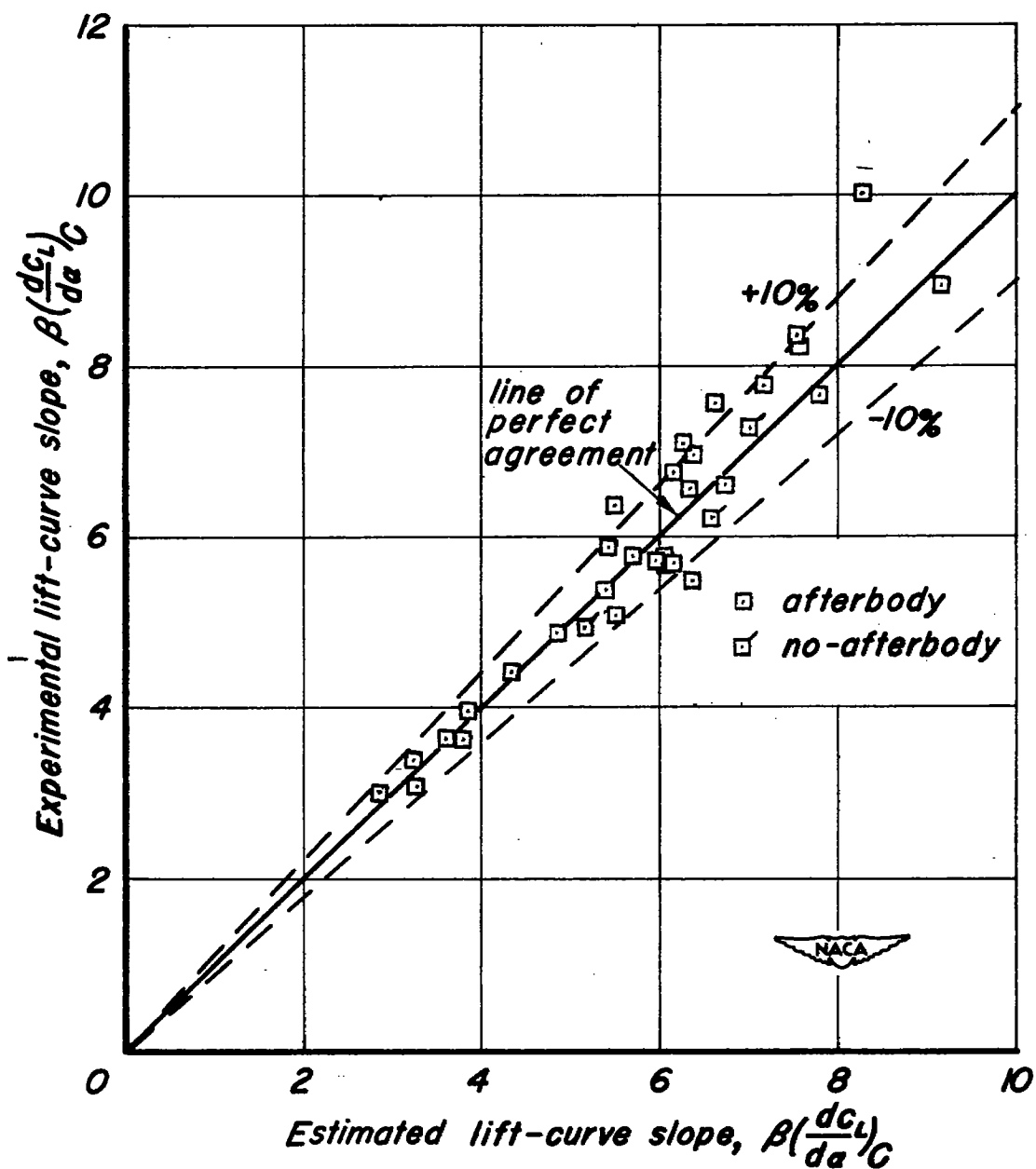
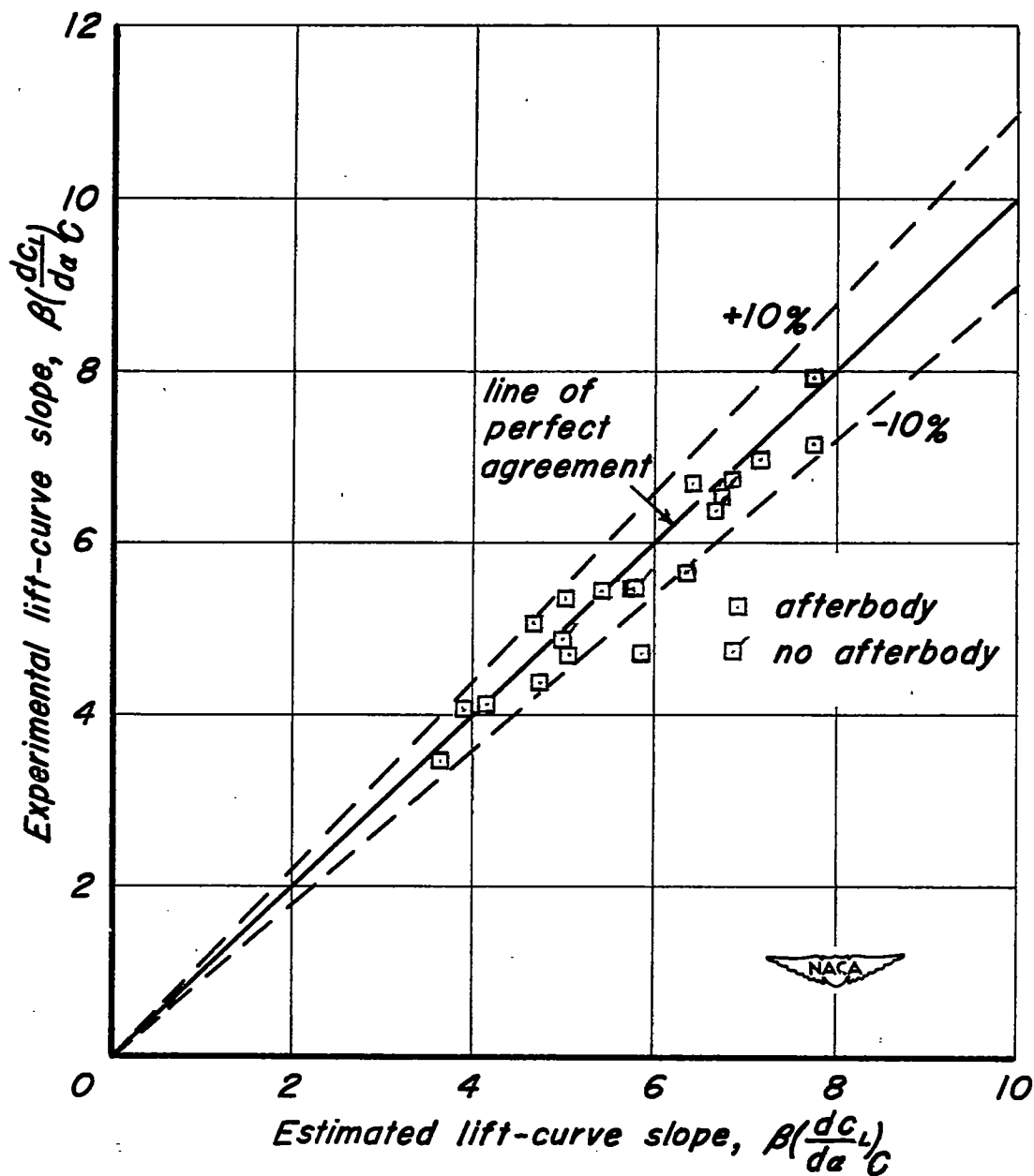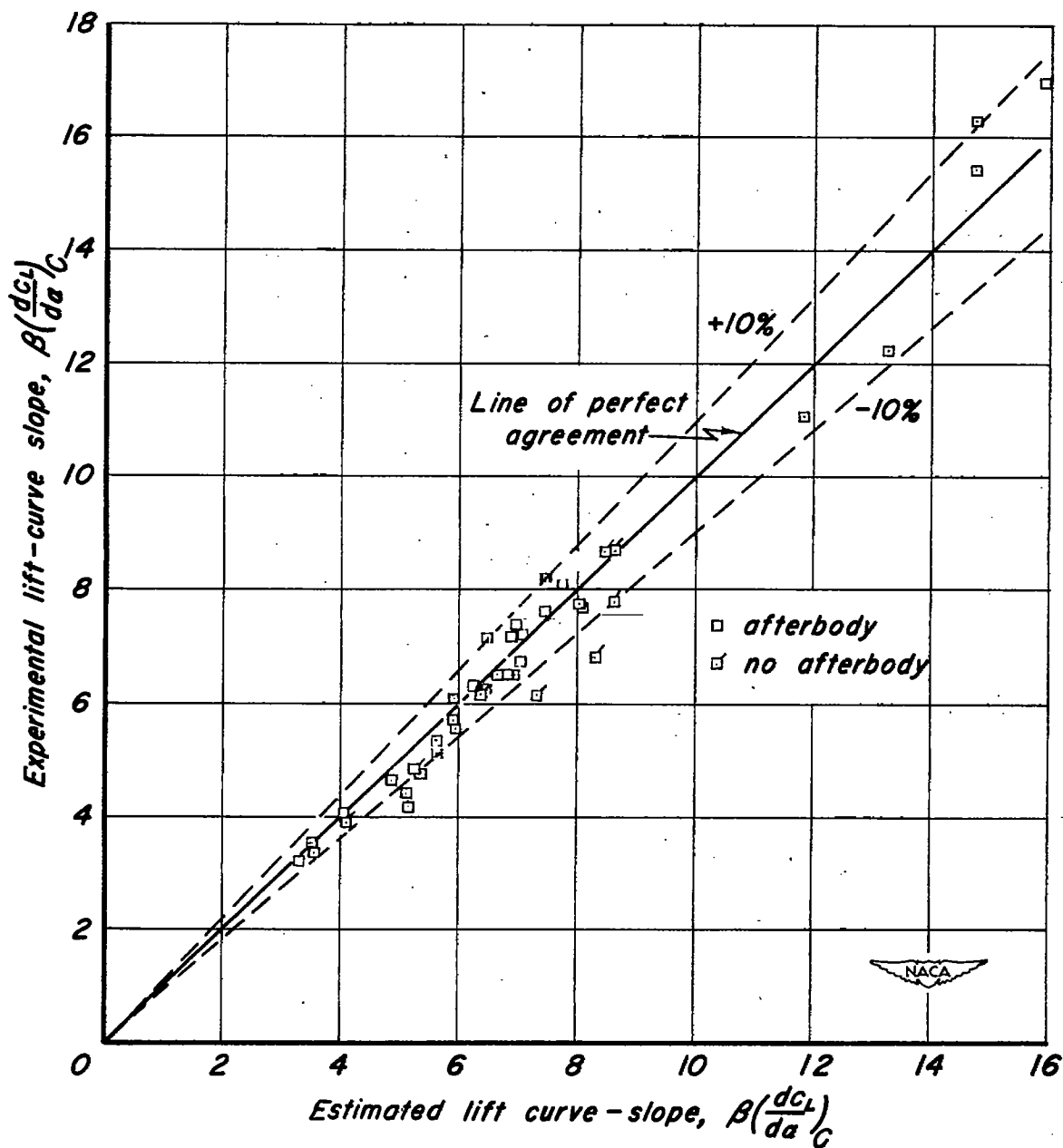Figure 6.— Correlation between experimental and estimated lift-curve slopes for triangular wing-body combinations.

Figure 7.— Correlation between experimental and estimated
lift-curve slopes for rectangular wing-body combinations.

Figure 8.— Correlation between experimental and estimated lift-curve
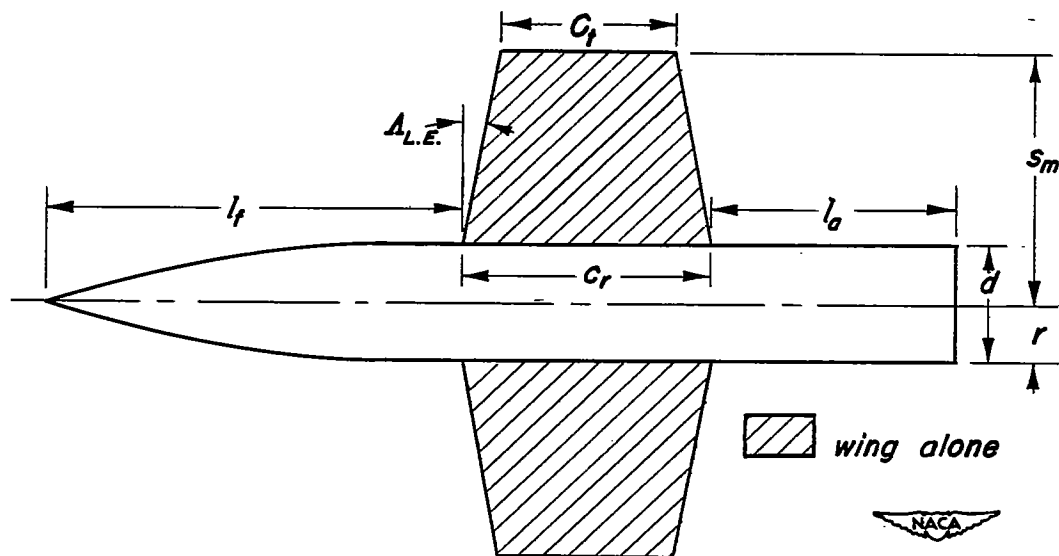slopes for trapezoidal wing-body combinations.

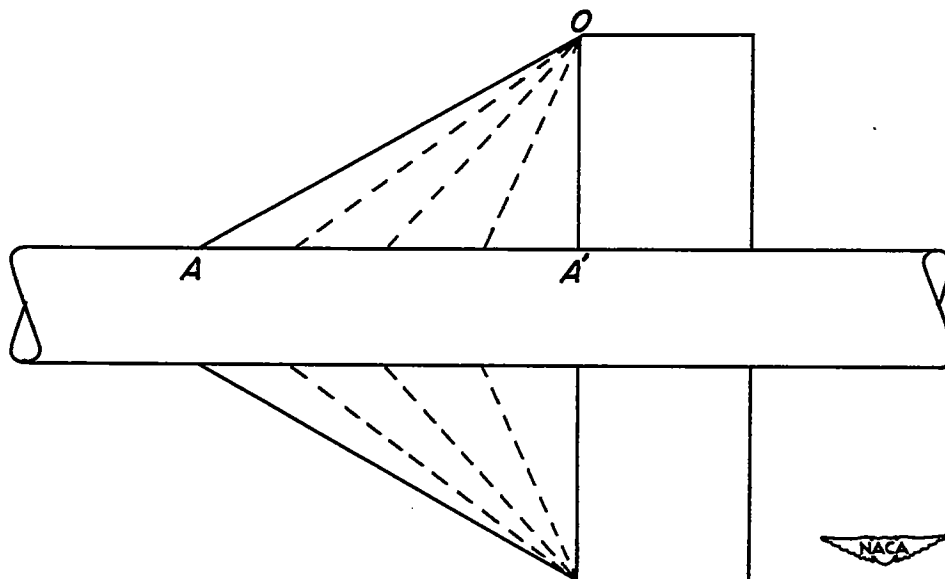Figure 9.- Plan form dimensions for wing-body combinations.

Figure 10.- Formation of rectangular wing-body combination from a slender combination.

UNAVAILABLE

UNAVAILABLE